


|   |  |                    |
|---|--|--------------------|
|  | <p align="center"><b>Study of AMV speed biases in the tropics</b></p> <p align="center"><b>Mid-term review report</b></p> <p align="center"><b>Results Task 1 - Task 3</b></p> |                    |
| Reference: AMV-TN-0004-TS_Ed1_Rev1  | Date : 17/04/2019  | Page : <i>i/59</i> |

# STUDY OF AMV SPEED BIASES IN THE TROPICS

## MID-TERM REVIEW REPORT

For: EUMETSAT  
 Addressee: Régis Borde  
 Reference: AMV-TN-0004-TS  
 Date: 17/04/2019  
 Edition: 1  
 Revision: 1  
 Page: *i/ 59*

### THALES Services SAS

290 allée du Lac  
 31670 Labège  
 France

Tel.: +33-562 88 86 00


Fax: +33-562 88 76 00

Web: <http://www.thalesgroup.com>



Division Secure Communications and Information Systems (SIX), 2019


Copyright 2019 - In accordance with EUMETSAT Contract No. EUM/CO/18/4600002168/RBo - Order n°4500017165

|   |  |                     |
|---|--|---------------------|
|  | <p align="center"><b>Study of AMV speed biases in the tropics</b></p> <p align="center"><b>Mid-term review report</b></p> <p align="center"><b>Results Task 1 - Task 3</b></p> |                     |
| Reference: AMV-TN-0004-TS_Ed1_Rev1  | Date : 17/04/2019  | Page : <i>ii/59</i> |

#### Evolution sheet


---

| Issue | Date       | Evolution                        | Reason for evolution   |
|-------|------------|----------------------------------|--|
| 1.1   | 17/04/2019 | Update following mid-term review | Correction of the comparison with MISR and minor corrections |
| 1.0   | 17/04/2019 | Creation                         |  |

|   |   |                      |
|---|---|----------------------|
|  | <p><b>Study of AMV speed biases in the tropics</b></p> <p><b>Mid-term review report</b></p> <p><b>Results Task 1 - Task 3</b></p> |                      |
| Reference: AMV-TN-0004-TS_Ed1_Rev1  | Date : 17/04/2019   | Page : <i>iii/59</i> |

Page blank for web publishing

---


|   |  |                     |
|---|--|---------------------|
|  | <p align="center"><b>Study of AMV speed biases in the tropics</b></p> <p align="center"><b>Mid-term review report</b></p> <p align="center"><b>Results Task 1 - Task 3</b></p> |                     |
| Reference: AMV-TN-0004-TS_Ed1_Rev1  | Date : 17/04/2019  | Page : <i>iv/59</i> |

## Summary

---

|          |   |           |
|----------|---|-----------|
| <b>1</b> | <b>INTRODUCTION .....</b>                                 | <b>11</b> |
| 1.1      | Purpose of the Document.....                              | 11        |
| 1.2      | References .....  | 11        |
| <b>2</b> | <b>DATA.....</b>  | <b>13</b> |
| 2.1      | AMV data .....  | 13        |
| 2.2      | Reference observations.....                               | 13        |
| <b>3</b> | <b>COMPARISON OF AMVS TO ECWMF WINDS .....</b>            | <b>15</b> |
| 3.1      | Comparison Methods.....                                   | 15        |
| 3.2      | Mean statistics .....                                     | 15        |
| 3.2.1    | AMVs from Meteosat-10 EUMETSAT (Met10EUM) IR imagery..... | 15        |
| 3.2.2    | AMVs from Metop IR imagery.....                           | 27        |
| <b>4</b> | <b>COMPARISON OF AMV TO REFERENCE OBSERVATIONS .....</b>  | <b>32</b> |
| 4.1      | MISR stereo AMV .....                                     | 32        |
| 4.2      | RAOB winds .....  | 35        |
| 4.3      | CALIPSO cloud top heights.....                            | 36        |
| 4.4      | CLOUDSAT cloud type classification .....                  | 38        |
| 4.5      | OLR .....   | 39        |
| 4.5.1    | Accumulated OLR from ECMWF.....                           | 39        |
| 4.5.2    | OLR from AIRS.....  | 43        |
| 4.5.3    | OLR from FY2E/FY2G.....                                   | 43        |
| 4.6      | GDI .....   | 46        |
| 4.6.1    | GDI from ECMWF.....                                       | 47        |
| 4.6.2    | GDI from ATOVS.....                                       | 47        |
| <b>5</b> | <b>SEMIVARIOGRAM .....</b>                                | <b>52</b> |
| 5.1      | Method .....  | 52        |
| 5.2      | Results .....   | 52        |
| <b>6</b> | <b>SUMMARY AND CONCLUSIONS .....</b>                      | <b>59</b> |



|   |  |                    |
|---|--|--------------------|
|  | <p align="center"><b>Study of AMV speed biases in the tropics</b></p> <p align="center"><b>Mid-term review report</b></p> <p align="center"><b>Results Task 1 - Task 3</b></p> |                    |
| Reference: AMV-TN-0004-TS_Ed1_Rev1  | Date : 17/04/2019  | Page : <b>v/59</b> |

## List of Figures

|   |    |
|---|----|
| Figure 1 : Geographic distribution of tropical Met10EUM wind speeds averaged for high levels ( $p \leq 400$ hPa) and over a $2^\circ \times 2^\circ$ latitude x longitude grid. Collocation criteria as described in Sec. 3.1 are used. ....                                  | 16 |
| Figure 2 : Geographic distribution of tropical ECMWF wind speeds averaged for high levels ( $p \leq 400$ hPa) and over a $2^\circ \times 2^\circ$ latitude x longitude grid. Only data collocated with Met10EUM AMVs are used. ....   | 17 |
| Figure 3 : Geographic distribution of tropical Met10EUM wind speeds against collocated ECMWF winds. O-B bias is averaged for high levels ( $p \leq 400$ hPa) and over a $2^\circ \times 2^\circ$ latitude x longitude grid. 18  |    |
| Figure 4 : Pressure assigned to Met10EUM AMV ( $p_{AMV}$ ) vs collocated best-fit pressure ( $p_{best-fit}$ ). Differences $p_{AMV} - p_{best-fit}$ are averaged for high-level winds ( $p \leq 400$ hPa) and over a $2^\circ \times 2^\circ$ latitude x longitude grid. .... | 19 |
| Figure 5 : Diurnal cycle of Met10EUM O-B speed bias for three zonal bands ( $35^\circ\text{S}$ - $15^\circ\text{S}$ , $15^\circ\text{S}$ - $15^\circ\text{N}$ , $15^\circ\text{N}$ - $35^\circ\text{S}$ ) and high-level winds. ....  | 20 |
| Figure 6 : As Figure 5, but only positive Met10EUM-ECMWF wind speed differences are used.....   | 21 |
| Figure 7 : As Figure 5, but only negative Met10EUM-ECMWF wind speed differences are used. ....  | 21 |
| Figure 8 : As Figure 3, but for mid-level winds ( $400 \text{ hPa} < p \leq 700 \text{ hPa}$ ). ....  | 22 |
| Figure 9 : Pressure assigned to Met10EUM AMV ( $p_{AMV}$ ) vs collocated best-fit pressure ( $p_{best-fit}$ ). As Fig. 4 but differences $p_{AMV} - p_{best-fit}$ are averaged for mid-level winds ( $400 \text{ hPa} < p \leq 700 \text{ hPa}$ ). ....                       | 23 |
| Figure 10 : Diurnal cycle of Met10EUM O-B speed bias for three zonal bands ( $35^\circ\text{S}$ - $15^\circ\text{S}$ , $15^\circ\text{S}$ - $15^\circ\text{N}$ , $15^\circ\text{N}$ - $35^\circ\text{S}$ ) and mid-level winds. ....  | 24 |
| Figure 11 : As Figure 3, but for low-level winds ( $p > 700 \text{ hPa}$ ). ....  | 25 |
| Figure 12 : Pressure assigned to Met10EUM AMV ( $p_{AMV}$ ) vs collocated best-fit pressure ( $p_{best-fit}$ ). As Figure 4, but differences $p_{AMV} - p_{best-fit}$ are averaged for mid-level winds ( $p > 700 \text{ hPa}$ ). ....  | 26 |
| Figure 13 : Diurnal cycle of Met10EUM's O-B speed bias for three zonal bands ( $35^\circ\text{S}$ - $15^\circ\text{S}$ , $15^\circ\text{S}$ - $15^\circ\text{N}$ , $15^\circ\text{N}$ - $35^\circ\text{S}$ ) and low-level winds. ....  | 27 |
| Figure 14 : Geographic distribution of tropical Metop wind speed against collocated ECMWF winds. O-B bias is averaged for high levels ( $p \leq 400$ hPa) and over a $2^\circ \times 2^\circ$ latitude x longitude grid.....  | 28 |
| Figure 15 : Geographic distribution of tropical Metop wind speeds averaged for high levels ( $p \leq 400$ hPa) and over a $2^\circ \times 2^\circ$ latitude x longitude grid. Collocation criteria as described in Sec. 3.1 are used. ....                                    | 28 |
| Figure 16 : Pressure assigned to Metop AMV ( $p_{AMV}$ ) vs collocated best-fit pressure ( $p_{best-fit}$ ). Differences $p_{AMV} - p_{best-fit}$ are averaged for high levels ( $p \leq 400$ hPa) and over a $2^\circ \times 2^\circ$ lat x lon grid. ....                   | 29 |


|   |  |              |
|---|--|--------------|
|  | <p align="center"><b>Study of AMV speed biases in the tropics</b></p> <p align="center"><b>Mid-term review report</b></p> <p align="center"><b>Results Task 1 - Task 3</b></p> |              |
| Reference: AMV-TN-0004-TS_Ed1_Rev1  | Date : 17/04/2019  | Page : vi/59 |

Figure 17 : Geographic distribution of Metop wind speed against collocated ECMWF winds. O-B bias is averaged for mid-levels ( $400 \text{ hPa} < p \leq 700 \text{ hPa}$ ) and over a  $2^\circ \times 2^\circ$  latitude x longitude grid. .... 29

Figure 18 : Geographic distribution of tropical Metop wind speeds averaged for mid levels ( $400 \text{ hPa} < p \leq 700 \text{ hPa}$ ) and over a  $2^\circ \times 2^\circ$  latitude x longitude grid. Collocation criteria as described in Sec. 3.1 are used. .... 30

Figure 19 : Pressure assigned to Metop AMV ( $p_{\text{AMV}}$ ) vs collocated best-fit pressure ( $p_{\text{best-fit}}$ ). Differences  $p_{\text{AMV}} - p_{\text{best-fit}}$  are averaged for mid-levels ( $400 \text{ hPa} < p \leq 700 \text{ hPa}$ ) and over a  $2^\circ \times 2^\circ$  latitude x longitude grid. .... 30

Figure 20 : Geographic distribution of tropical Metop wind speed against collocated ECMWF winds. O-B bias is averaged for low levels ( $p > 700 \text{ hPa}$ ) and over a  $2^\circ \times 2^\circ$  latitude x longitude grid. .... 31

Figure 21 : Monthly profiles of mean differences between Met10EUM AMV and MISR wind speeds (red line) and corresponding standard deviation (light red shades). .... 33

Figure 22 : Monthly profiles of mean differences between Metop AMV and MISR wind speeds (red line) and corresponding standard deviation (light red shades). .... 34

Figure 23 : Geographic distribution of tropical Metop wind speeds against MISR winds averaged for high levels ( $p \leq 400 \text{ hPa}$ ) and over a  $5^\circ \times 5^\circ$  latitude x longitude grid. Collocation criteria as described in Sec. 4.1 are used. .... 35

Figure 24 : Profile of mean Metop-RAOB wind speed differences (blue) and corresponding standard deviation (blue shaded area). RAOB were collocated with Metop using criteria introduced in Sec. 3. . 36

Figure 25 : Comparison of CALIPSO cloud top height with Met10EUM AMVs. Box-and-whisker plots of AMV-CALIPSO pressure ( $p_{\text{AMV}} - p_{\text{CALIPSO}}$ ) difference are shown for different AMV pressure levels, whereby each box contains data in a pressure range of 50 hPa. Each box extends from the lower to upper quartile values of the pressure differences, with a red line at the median. Corresponding O-B speed bias is shown in blue, while corresponding ECMWF speeds are shown in red. Numbers in the left part of each figure denote the number of collocations used to calculate pressure differences. No CALIPSO data were available for February 2016. .... 37

Figure 26 : Correlation of CLOUDSAT cloud types with observed O-B speed bias of Met10EUM AMVs against ECMWF winds for (a) high-level clouds, (b) mid-level and (c) low-level clouds. Horizontal blue lines denote mean wind speed differences Met10EUM AMV - ECMWF, while vertical blue lines denote the corresponding standard deviation. CLOUDSAT groups clouds into cirrus (1), altostratus (2), altocumulus (3), stratus (4), stratocumulus (5), cumulus (6, including cumulus congestus), nimbostratus (7) and deep convection (8). Depicted are also geographical distribution of CLOUDSAT and Met10EUM AMV collocations for (d) high-level clouds, (e) mid-level and (f) low-level clouds. Results for 8 months averages are presented (January to August). .... 39

Figure 27 : Comparison of ECMWF OLR (step range = 1, see text) with Met10EUM AMVs. Box-and-whisker plots of OLR are shown for different AMV pressure levels. Each box extends from the lower to upper quartile values of the pressure differences, with a line at the median. Corresponding O-B speed bias is shown in blue, while ECMWF speeds are shown in red. .... 41

Figure 28 : As Figure 27, but for Metop AMVs. .... 42


|   |  |                      |
|---|--|----------------------|
|  | <p align="center"><b>Study of AMV speed biases in the tropics</b></p> <p align="center"><b>Mid-term review report</b></p> <p align="center"><b>Results Task 1 - Task 3</b></p> |                      |
| Reference: AMV-TN-0004-TS_Ed1_Rev1  | Date : 17/04/2019  | Page : <i>vii/59</i> |

Figure 29 : Comparison of AIRS OLR with Met10EUM AMVs. Black horizontal lines denote the mean OLR plus corresponding standard deviations. Corresponding O-B speed bias (Met10EUM-ECMWF) is shown in blue, while collocated ECMWF wind speed is shown in red..... 44

Figure 30 : As Figure 29, but for AIRS OLR and Metop AMV. .... 45

Figure 31 : As Fig. 30 but for collocated OLR and AMV from FY2G and FY2E, respectively. (Left) Mean and standard deviation of matched FY2G OLR vs FY2G AMV-ECMWF in December 2016. (Right) Mean and standard deviation of matched FY2E OLR vs FY2E AMV-ECMWF in June 2016. .... 46

Figure 32 : Correspondence between GDI values and expected type of convection. Figure adapted from <http://www.wpc.ncep.noaa.gov/international/gdi/> ..... 47

Figure 33 : Comparison of ECMWF GDI with Met10EUM AMVs. Box-and-whisker plots of GDI are shown for different AMV pressure levels. Each box extends from the lower to upper quartile values of the pressure differences, with a line at the median. Corresponding O-B speed bias is shown in blue, while ECMWF speeds are shown in red. The grey vertical stripes denotes the border of the different convective regimes according to Figure 32. .... 48

Figure 34 : As Figure 33, but for Metop AMVs. .... 49

Figure 35 : Comparison of ATOVS GDI with Met10EUM AMVs. Black horizontal lines denote the mean GDI values plus corresponding standard deviations. Corresponding O-B speed bias (Met10EUM-ECMWF) is shown in blue, while ECMWF speed is shown in red. The grey vertical stripes denotes the border of the different convective regimes according to Figure 32. .... 50

Figure 36 : As Figure 35, but for Metop AMVs. .... 51


Figure 37 : Geographic distribution of tropical Met10EUM wind speeds against collocated ECMWF winds for March 2016. (Left) O-B bias is averaged for high levels ( $p \leq 400$  hPa) and over a  $2^\circ \times 2^\circ$  latitude x longitude grid. Black square indicates a region of large wind speed discrepancies. (Right) Monthly averages of Met10EUM AMV and ECWMF wind speed for high-level, mid-level and low-level winds for the black square and its surrounding are depicted. .... 53

Figure 38 : Semivariograms and histograms of Met10EUM AMV and model wind for different pressure levels for the black square region of Figure 37. (Upper panel) Semivariance  $\gamma$  for AMV (blue) and model wind (black) as function of lag distance  $h$  for selected pressure levels. (Lower panel) Corresponding histograms of AMV (blue) and model wind (black). The numbers indicate the mean of the histograms (blue for AMV histogram, black for model wind), and observed O-B speed bias (AMV-Model). # denotes the sample size. .... 54

Figure 39 : Geographic distribution of tropical Met10EUM wind speeds against collocated ECMWF winds for January 2016. (Left) O-B bias is averaged for high levels ( $p \leq 400$  hPa) and over a  $2^\circ \times 2^\circ$  latitude x longitude grid. Black square indicates a region of large wind speed discrepancies. (Right) Monthly averages of Met10EUM AMV and ECWMF wind speed for high-level, mid-level and low level winds for the black square and its surrounding. .... 55

Figure 40 : As Figure 38, but for the black square region of Figure 39. .... 56

Figure 41 : Geographic distribution of tropical Metop wind speeds against col-located ECMWF winds for December 2016. (Top) O-B bias is averaged for high levels ( $p \leq 400$  hPa) and over a  $2^\circ \times 2^\circ$  latitude

|   |  |                       |
|---|--|-----------------------|
|  | <p align="center"><b>Study of AMV speed biases in the tropics</b></p> <p align="center"><b>Mid-term review report</b></p> <p align="center"><b>Results Task 1 - Task 3</b></p> |                       |
| Reference: AMV-TN-0004-TS_Ed1_Rev1  | Date : 17/04/2019  | Page : <i>viii/59</i> |

x longitude grid. Black square over Indonesia indicates a region of large wind speed discrepancies. (Bottom) Monthly averages of Metop AMV and ECWMF wind speed for high-level, mid-level and low level winds for the black square and its surrounding ..... 57

Figure 42 : As Figure 38, but for the black square region of Figure 41. .... 58


## List of Tables

---

Table 1 : Overview of AMV data sets used in this study..... 13


Table 2: Overview of reference data sets used in this study. T denotes temperature, q specific humidity and OLR outgoing longwave radiation..... 14

Table 3 : Overview RAOB data availability in tropics (latitudes  $\leq \pm 35^\circ$ ) for 2016. Number of radiosondes are grouped into Western Pacific ( $90^\circ\text{E} < \text{longitude} \leq 150^\circ\text{E}$ ), Indian Ocean ( $45^\circ\text{E} < \text{longitude} \leq 90^\circ\text{E}$ ) and Africa ( $-50^\circ\text{E} < \text{longitude} \leq 45^\circ\text{E}$ ). .... 35


|   |  |                     |
|---|--|---------------------|
|  | <p align="center"><b>Study of AMV speed biases in the tropics</b></p> <p align="center"><b>Mid-term review report</b></p> <p align="center"><b>Results Task 1 - Task 3</b></p> |                     |
| Reference: AMV-TN-0004-TS_Ed1_Rev1  | Date : 17/04/2019  | Page : <i>ix/59</i> |

## Abbreviations

|                 |  |
|-----------------|--|
| <b>AIRS</b>     | Atmospheric Infrared Sounder   |
| <b>AMSU</b>     | Copernicus Atmosphere Monitoring Service                                     |
| <b>AMV</b>      | Atmospheric Motion Vector  |
| <b>ATOVS</b>    | Advanced microwave sounding unit   |
| <b>AVHRR</b>    | Advanced very-high-resolution radiometer                                     |
| <b>AWX</b>      | Advanced Weather-satellite eXchange format                                   |
| <b>CALIPSO</b>  | Cloud-Aerosol Lidar and Infrared Pathfinder Satellite Observations satellite |
| <b>CIMSS</b>    | Cooperative Institute for Meteorological Satellite Studies                   |
| <b>EUMETSAT</b> | European Organisation for the Exploitation of Meteorological Satellites      |
| <b>EOP</b>      | EUMETSAT's Earth Observation Portal  |
| <b>GOES</b>     | Geostationary Operational Environmental Satellite                            |
| <b>GDI</b>      | Galvez-Davison Index   |
| <b>GRIB</b>     | GRIdded Binary data format   |
| <b>HDF-EOS</b>  | Hierarchical Data Format – Earth Observing System                            |
| <b>HIRS</b>     | High-resolution Infrared Radiation Sounder                                   |
| <b>IFS</b>      | Integrated Forecast System   |
| <b>IGRA</b>     | Integrated Global Radiosonde Archive   |
| <b>MHS</b>      | Microwave Humidity Sounder   |
| <b>MISR</b>     | Multi-angle Imaging SpectroRadiometer,                                       |
| <b>NASA</b>     | National Aeronautics and Space Administration                                |
| <b>NOAA</b>     | National Oceanic and Atmospheric Administration                              |
| <b>NSMC</b>     | Chinese National Satellite Meteorological Center                             |

|   |  |                    |
|---|--|--------------------|
|  | <p align="center"><b>Study of AMV speed biases in the tropics</b></p> <p align="center"><b>Mid-term review report</b></p> <p align="center"><b>Results Task 1 - Task 3</b></p> |                    |
| Reference: AMV-TN-0004-TS_Ed1_Rev1  | Date : 17/04/2019  | Page : <b>x/59</b> |

|             |   |
|-------------|---|
| <b>NWP</b>  | Numerical Weather Prediction  |
| <b>O-B</b>  | Observation-Background. Here wind speed difference between observed wind (AMV) and model wind (ECMWF) |
| <b>OLR</b>  | Outgoing Longwave Radiation   |
| <b>QI</b>   | Quality index/indicator   |
| <b>RAOB</b> | RAdiosonde OBservation  |
| <b>TOA</b>  | Top-of-atmosphere   |
| <b>TTR</b>  | Top thermal radiation   |

|   |  |              |
|---|--|--------------|
|  | <p align="center"><b>Study of AMV speed biases in the tropics</b></p> <p align="center"><b>Mid-term review report</b></p> <p align="center"><b>Results Task 1 - Task 3</b></p> |              |
| Reference: AMV-TN-0004-TS_Ed1_Rev1  | Date : 17/04/2019  | Page : 11/59 |

# 1 INTRODUCTION


## 1.1 PURPOSE OF THE DOCUMENT

This document constitute the mid-term review report of the study "*Study of AMV speed biases in the tropics*" ([DR1]) and comprises of the results of Task 1 - Task 3. In Sec. 2 the AMV data and reference observations are specified, including provider, file format, gaps and other specificities of the data. In this sense, Sec. 2 summarizes Task 1 of Thales' Technical and Management Proposal ([DR2]). Section 3 describes the method to collocate AMVs to forecast wind fields from ECWMF and presents mean statistics averaged for high, mid and low levels. Section 3 thus forms Task 2 of Thales' proposal. An important aspect of this Task 2 comprises of establishing a collocation database (of ECMWF winds and AMVs) upon which results of succeeding analysis are based. Section 4 uses the established collocation data base to relate Observation-Background (O-B) speed biases to other parameters such as OLR or cloud types and forms Task 3 of Thales' proposal. Lastly, semivariograms are applied to selected cases to investigate similarities/discrepancies in collocated wind fields (Sec. 5). Results will be presented for selected cases.

Results are mainly presented for AMVs derived from Metop and Meteosat-10 IR imagery by EUMETSAT as these data are exhibit high temporal result ion and quality indicators are provided. Results for the other AMV datasets and channel/satellite combinations are presented in less detail in a separate document.


## 1.2 REFERENCES

| Number | Reference   | Document title  |
|--------|---|---|
| [DR1]  | EUM/TSS/SOW/16/849154<br>v1A, 15 February 2018<br>Study_of_AMV_speed_biases_in_the_tropics_EUMITS_1003067 | Study of AMV speed biases in the tropics  |
| [DR2]  | THALES. Ref: 351100-18-PTE-0214-TS  | Technical and Management Proposal. Study of AMV speed biases in the tropics.                                      |
| [DR3]  | Folger, K., and M. Weissmann, 2014, J. Appl. Meteor. Climatol., 53, 1809-1819                             | Height correction of atmospheric motion vectors using satellite lidar observations from CALIPSO.                  |
| [DR4]  | Gálvez, J.M. and Davison, M., 2016:   | The Gálvez-Davison Index for Tropical Convection. National Oceanic and Atmospheric Administration. 23 pp.         |
| [DR5]  | Hogan, 2014   | Radiation Quantities in the ECMWF model and MARS  |
| [DR6]  | Horvath, A., and Davies, R., 2001, J. Atmos. Oceanic Technol., 18, 591-608                                | Feasibility and error analysis of cloud motion wind extraction from near-simultaneous multiangle MISR measurement |
| [DR7]  | Horváth, Á., O. Hautecoeur, R. Borde, H. Deneke, and S.A. Buehler, 2017                                   | Evaluation of the EUMETSAT Global AVHRR Wind Product  |

|   |  |              |
|---|--|--------------|
|  | <p align="center"><b>Study of AMV speed biases in the tropics</b></p> <p align="center"><b>Mid-term review report</b></p> <p align="center"><b>Results Task 1 - Task 3</b></p> |              |
| Reference: AMV-TN-0004-TS_Ed1_Rev1  | Date : 17/04/2019  | Page : 12/59 |

| Number        | Reference   | Document title  |
|---------------|---|---|
|               | J. Appl. Meteor. Climatol., 56, 2353–2376. doi: <a href="https://doi.org/10.1175/JAMC-D-17-0059.1">https://doi.org/10.1175/JAMC-D-17-0059.1</a> |   |
| <b>[DR8]</b>  | Salonen, K., Cotton, J., Bormann, N., & Forsythe, M., 2015: Journal of Applied Meteorology and Climatology, 54(1), 225-242.                     | Characterizing AMV Height-Assignment Error by Comparing Best-Fit Pressure Statistics from the Met Office and ECMWF Data Assimilation Systems. |
| <b>[DR9]</b>  | Weissmann, M., K. Folger and H. Lange, 2013: J. Appl. Meteor. Climatol., 52, 1868–1877.   | Height correction of atmospheric motion vectors using airborne lidar observations.  |
| <b>[DR10]</b> | Yang, G.Y. and J. Slingo, 2000. Monthly Weather Review, 129, 784-801.   | The Diurnal Cycle in the Tropics  |



|   |  |              |
|---|--|--------------|
|  | <p align="center"><b>Study of AMV speed biases in the tropics</b></p> <p align="center"><b>Mid-term review report</b></p> <p align="center"><b>Results Task 1 - Task 3</b></p> |              |
| Reference: AMV-TN-0004-TS_Ed1_Rev1  | Date : 17/04/2019  | Page : 13/59 |

## 2 DATA

### 2.1 AMV DATA

Given the decision taken during the Kickoff meeting held on November 8, 2016, AMV data were collected for 2016. The choice of this year was justified by analysing most recent AMV extraction schemes and by the availability CLOUDSAT data. Table 1 provides an overview of AMV data sets used in this study. Global Metop dual-mode AMVs, Meteosat-10 AMVs (Met10EUM) as well as Expanded Low-resolution Cloud Motion Winds from Meteosat-7 (Met7EUM, 57°E) were downloaded from the EUMETSAT Observation Portal (EOP; <https://eoportal.eumetsat.int/userMgmt/login.faces>).


**Table 1 : Overview of AMV data sets used in this study**

| Data set provider | AMV data set | Label    | Data format |
|-------------------|--------------|----------|-------------|
| EUMETSAT          | Metop        | Metop    | EPS Native  |
| EUMETSAT          | Meteosat-10  | Met10EUM | bufr        |
| EUMETSAT          | Meteosat-7   | Met7EUM  | bufr        |
| CIMSS             | GOES-13      | GOES13   | ascii       |
| CIMSS             | GOES-15      | GOES15   | ascii       |
| CIMSS             | Meteosat-7   | MET7     | ascii       |
| CIMSS             | Meteosat-10  | MET10    | ascii       |
| NSMC              | FY2E         | FY2E     | awx         |
| NSMC              | FY2G         | FY2G     | awx         |

Data sets from the geostationary satellites GOES-13, GOES-15, Meteosat-7 and Meteosat-10 were obtained from the wind archives of the University of Wisconsin-Madison Cooperative Institute for Meteorological Satellite Studies (CIMSS). These data are typically available on a 3-hourly basis. Finally, AMVs derived from the Chinese satellites FY2E and FY2G were obtained from the Chinese National Satellite Meteorological Center (NSMC). These data are stored in binary format awx (Advanced Weather-satellite eXchange format) and are available on a 3-hourly basis. AMVs from NSMC do not provide quality indicators.

### 2.2 REFERENCE OBSERVATIONS

In Sec. 3, these AMVs are compared to gridded wind fields from ECMWF's Integrated Forecast System (Table 2). We used hourly forecast data (from two runs, 00 and 12 UTC) at a horizontal resolution of 0.5° x 0.5° at 19 discrete pressure level (20, 30, 50, 70, 100 to 300 by 50, 400 to 800 by 100, 850, 900, 925, 950, 1000 hPa). AMVs were also compared to winds from radiosonde observations and to MISR stereo AMVs. The former data set was downloaded from an IGRA ftp server (<ftp://ftp.ncdc.noaa.gov/pub/data/igra/data/data-y2d/>). The number of available radiosondes in the tropics varies strongly among the different years and regions. MISR AMVs were downloaded from NASA ([https://eosweb.larc.nasa.gov/project/misr/mi3mcmvn\\_table](https://eosweb.larc.nasa.gov/project/misr/mi3mcmvn_table)) as monthly-aggregated Cloud Motion Vector Product. We used the most recent version F02 0002.

|   |  |              |
|---|--|--------------|
|  | <p align="center"><b>Study of AMV speed biases in the tropics</b></p> <p align="center"><b>Mid-term review report</b></p> <p align="center"><b>Results Task 1 - Task 3</b></p> |              |
| Reference: AMV-TN-0004-TS_Ed1_Rev1  | Date : 17/04/2019  | Page : 14/59 |


Temperature and specific humidity profiles required for GDI computation were obtained from ATOVS, ECMWF's IFS and AIRS. ATOVS data were downloaded from EUMETSAT's EOP. ATOVS is composed of the Advanced Microwave Sounding Unit A (AMSU-A), the Microwave Humidity Sounder (MHS) and the High Resolution Infrared Radiation Sounder (HIRS/4) aboard Metop. T and q profiles from AIRS (and AMSU) aboard AQUA are obtained from [https://disc.gsfc.nasa.gov/datasets/AIRX2RET\\_V006/summary?keywords=airs%20version%206](https://disc.gsfc.nasa.gov/datasets/AIRX2RET_V006/summary?keywords=airs%20version%206). At the time of downloading, AIRS/AMSU data were available until September 2016. Temperature and humidity are also regularly reported by radiosondes. However, in 2016, no humidity data were reported from tropical radiosondes. Thus, no GDI could be computed from radiosondes.

**Table 2: Overview of reference data sets used in this study. T denotes temperature, q specific humidity and OLR outgoing longwave radiation.**

| Type                      | Data set provider | Data set    | Data format |
|---------------------------|-------------------|-------------|-------------|
| Reference wind            | ECMWF             | IFS         | grib        |
| Reference wind            | IGRA              | Radiosondes | ascii       |
| Reference wind            | NASA              | MISR        | netcdf      |
| T, q profiles             | EUMETSAT          | ATOVS       | bufr        |
| T, q profiles             | IGRA              | Radiosondes | ascii       |
| T, q profiles             | ECMWF             | IFS         | ascii       |
| T, q profiles             | NASA              | AIRS        | HDF-EOS     |
| Cloud top pressure        | NASA              | CALIPSO     | HDF-EOS     |
| OLR                       | NASA              | AIRS        | HDF-EOS     |
| OLR                       | ECMWF             | IFS         | grib        |
| OLR                       | NSMC              | FY2E        | awx         |
| OLR                       | NSMC              | FY2G        | awx         |
| Cloud type classification | NASA              | CLOUDSAT    | HDF-EOS     |

CALIPSO cloud top pressure were available and downloaded from NASA's EARTH DATA site. CLOUDSAT data are available until August 2016 and were downloaded from <http://www.cloudsat.cira.colostate.edu/order-data>.

OLR data were used from AIRS, ECMWF's IFS, FY2E and FY2G. OLR data from AIRS were included in the same data products as the T and q profiles. However, they were only available until September 24, 2016. OLR from FY2E and FY2G were obtained from NSMC in awx format. As for AMV, NSMC does not provide quality indicators for the OLR products. The net long-wave radiation (TTR) at TOA (top-of-atmosphere) was downloaded from ECMWF. TTR is equal to the negative of the outgoing long-wave radiation (i.e.  $OLR = -TTR$ , see Hogan, 2014).

|   |  |              |
|---|--|--------------|
|  | <p align="center"><b>Study of AMV speed biases in the tropics</b></p> <p align="center"><b>Mid-term review report</b></p> <p align="center"><b>Results Task 1 - Task 3</b></p> |              |
| Reference: AMV-TN-0004-TS_Ed1_Rev1  | Date : 17/04/2019  | Page : 15/59 |

## 3 COMPARISON OF AMVS TO ECWMF WINDS

### 3.1 COMPARISON METHODS

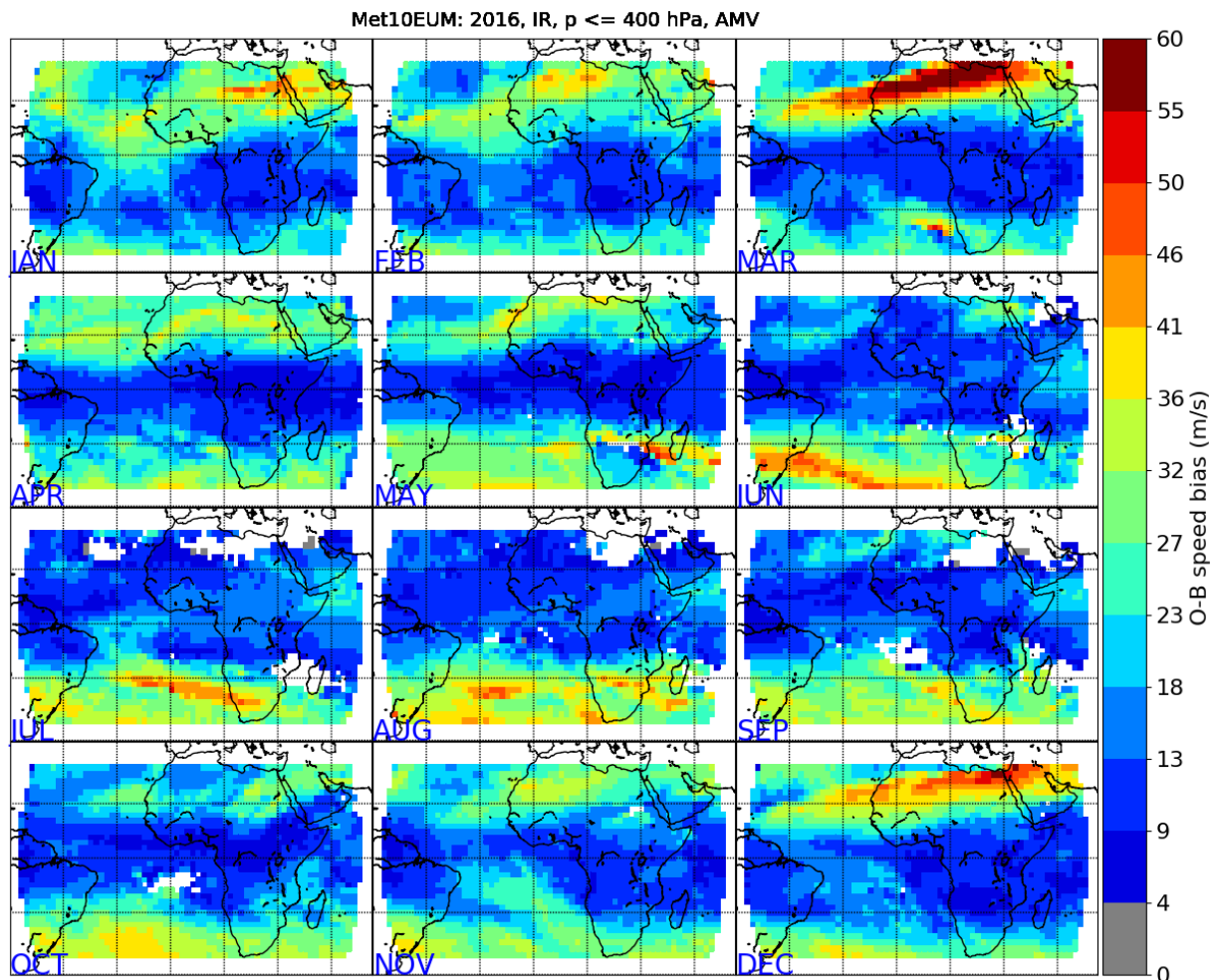
Comparison of AMVs to gridded wind fields from ECMWF requires establishing appropriate vertical and temporal collocation or match criteria. Horvath et al. (2017) is followed to establish appropriate match criteria, i.e., a vertical separation between ECMWF and AMV of less than 25 hPa ( $p \leq \pm 25$ hPa), a temporal separation of less than 30 min and a wind direction difference of less than  $60^\circ$  is required for comparison. It is possible that more than one AMV falls into the same ECMWF grid cell. If this is the case, the median of the concerned AMVs is calculated and compared to ECMWF winds.

With the exception of FY2G and FY2E winds, quality indicators (QI) are reported. In these cases, we considered only AMVs where the QI exceeds a value of 60 (polar satellites, i.e., Metop AMVs) and 80 (geostationary satellites), respectively. Results are presented as O-B speed bias (AMV-ECMWF) and typically separately for high-level winds ( $p \leq 400$  hPa), mid-level winds ( $400 \text{ hPa} < p \leq 700$  hPa) and low-level winds ( $p > 700$  hPa). To investigate height-assignment differences, the  $p \leq \pm 25$  hPa criterion is relaxed and AMV pressures are compared to so-called best-fit pressures. The best-pressure fit is defined as the height at which the vector difference between the observed and the model background wind is smallest. To calculate the best-fit pressure we follow Salonen et al. (2015), who suggest a two-step procedure to obtain best-fit pressure. The first step consists in finding the model level that minimizes the vector difference between AMV and model wind. The second step consists in calculating the "true minimum" by using a parabolic fit to the vector difference for this model level and the two neighbouring levels. Criteria used by Salonen et al. (2015) to eliminate cases for which the best-fit pressure is not well constrained are also applied (Eq. (1) and (2) in Salonen et al., 2015). That is, cases in which there is no good agreement between the AMV wind observation and the model wind at any level are excluded. Secondly, the vector difference must be greater than the minimum difference  $+ 2 \text{ ms}^{-1}$  outside a band that encompasses the best-fit pressure  $\pm 100$  hPa.

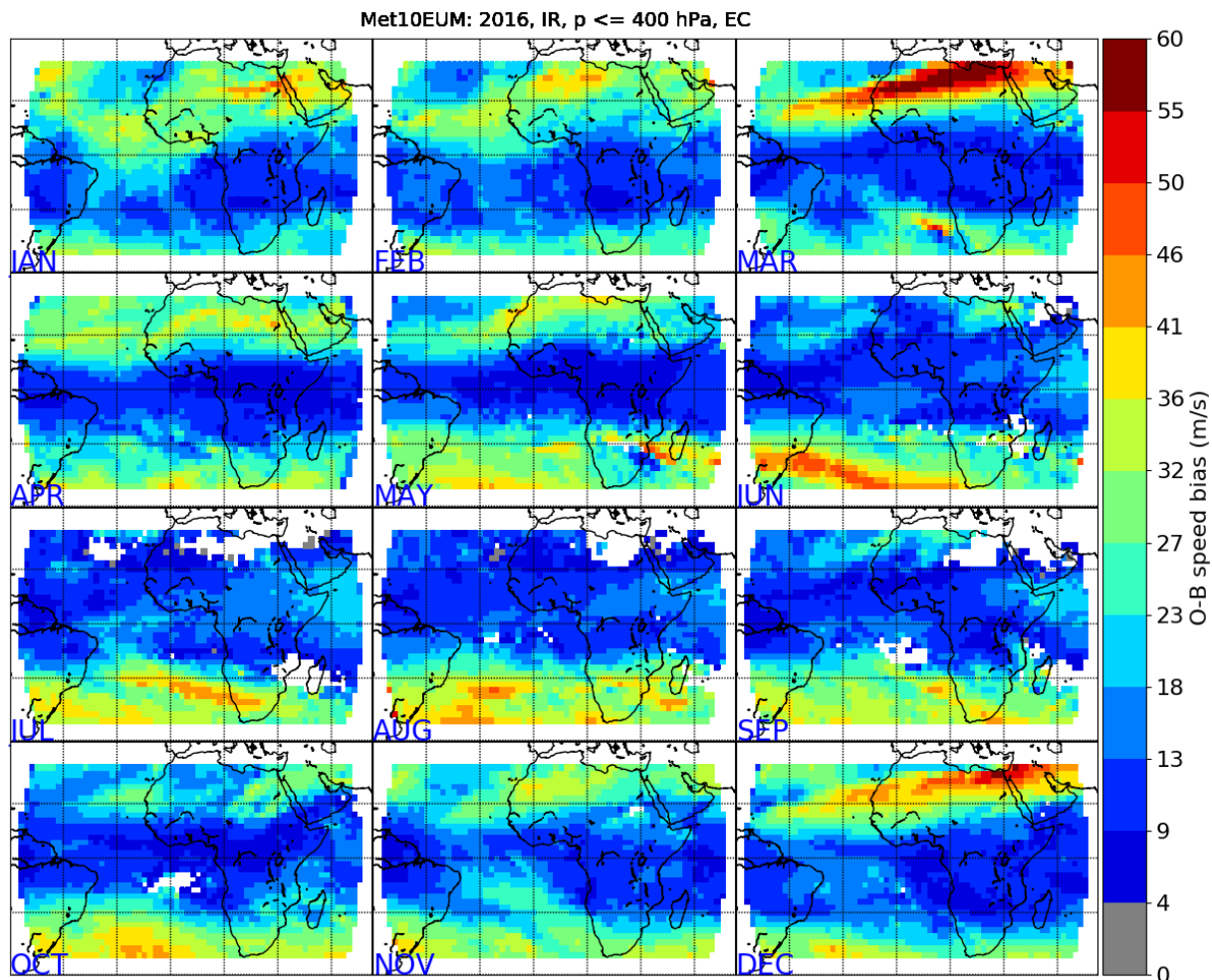
### 3.2 MEAN STATISTICS

#### 3.2.1 AMVs from Meteosat-10 EUMETSAT (Met10EUM) IR imagery

**High-level winds:** Monthly spatial distributions of wind speed derived by Met10EUM IR imagery and by ECMWF is given in Figure 1 and Figure 2 for high-level winds ( $p \leq 400$  hPa), respectively, while the spatial distribution of corresponding wind speed differences (Met10EUM - ECMWF) is given in Figure 3. Mean speed discrepancies are around  $1 \text{ ms}^{-1}$ . Areas of wind speed differences of greater than  $3 \text{ ms}^{-1}$  commonly coincide with the location the subtropical jet that migrates with the changing position of the thermal equator (e.g. high wind speeds over the Sahara desert in December to March, high wind speeds in Southern Africa from July to August). Negative mean wind differences larger than  $5 \text{ ms}^{-1}$  are often found over oceans, e.g. over the Gulf of Guinea in January or south of Madagascar in June).

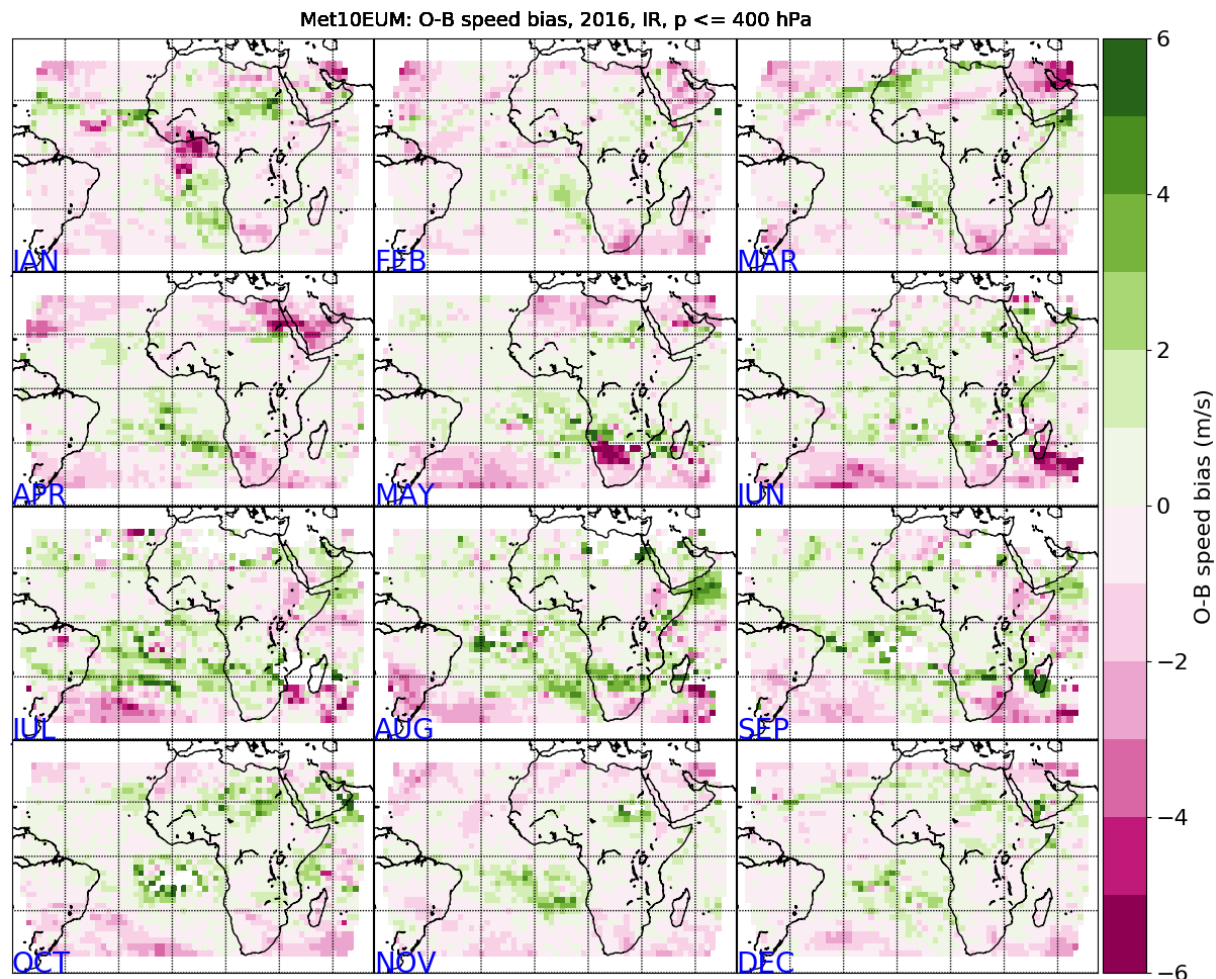


**Figure 1 : Geographic distribution of tropical Met10EUM wind speeds averaged for high levels ( $p \leq 400$  hPa) and over a  $2^\circ \times 2^\circ$  latitude x longitude grid. Collocation criteria as described in Sec. 3.1 are used.**




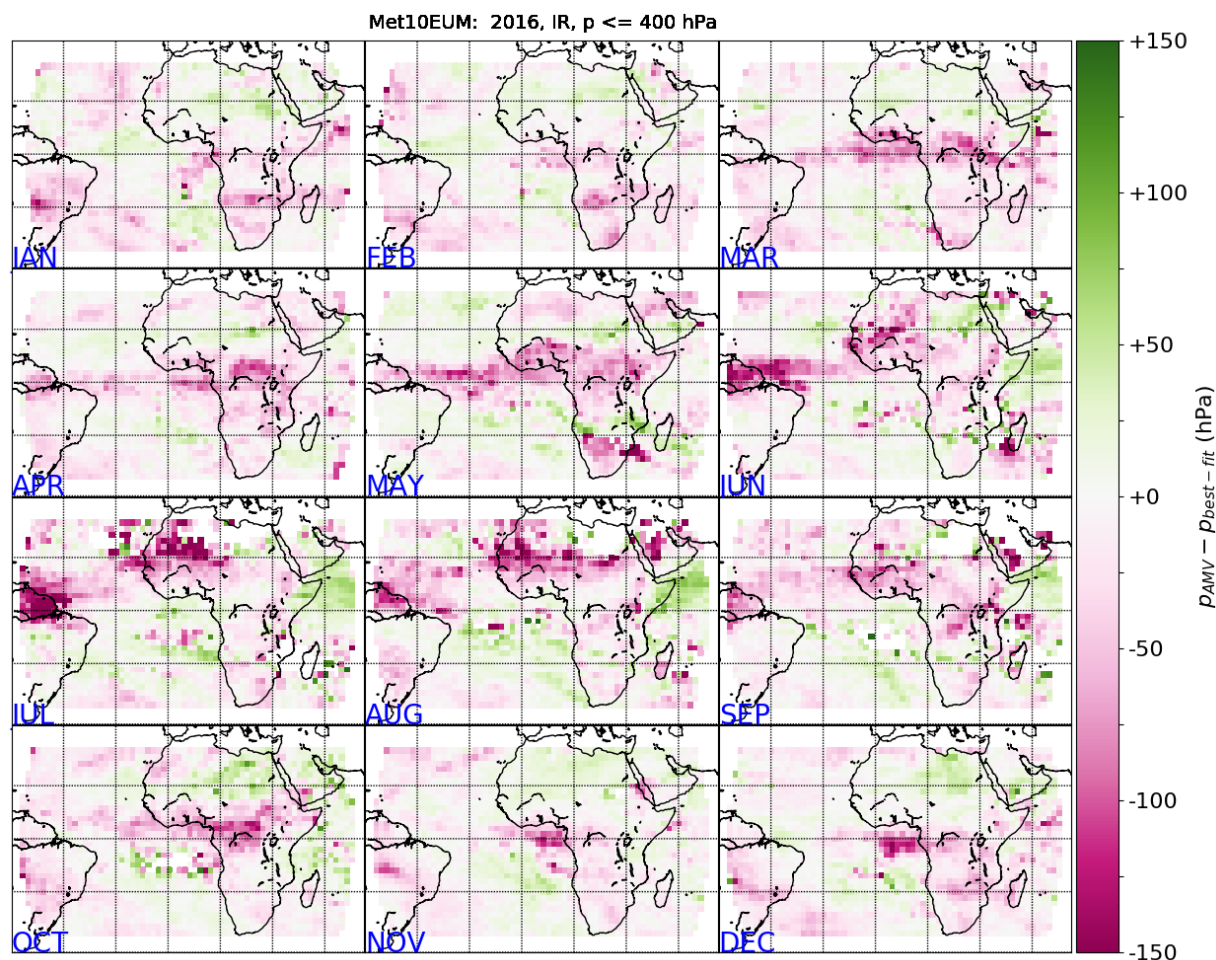
**Figure 2 : Geographic distribution of tropical ECMWF wind speeds averaged for high levels ( $p \leq 400$  hPa) and over a  $2^\circ \times 2^\circ$  latitude x longitude grid. Only data collocated with Met10EUM AMVs are used.**





**Figure 3 : Geographic distribution of tropical Met10EUM wind speeds against collocated ECMWF winds. O-B bias is averaged for high levels ( $p \leq 400$  hPa) and over a  $2^\circ \times 2^\circ$  latitude x longitude grid.**


|   |  |              |
|---|--|--------------|
|  | <p align="center"><b>Study of AMV speed biases in the tropics</b></p> <p align="center"><b>Mid-term review report</b></p> <p align="center"><b>Results Task 1 - Task 3</b></p> |              |
| Reference: AMV-TN-0004-TS_Ed1_Rev1  | Date : 17/04/2019  | Page : 19/59 |



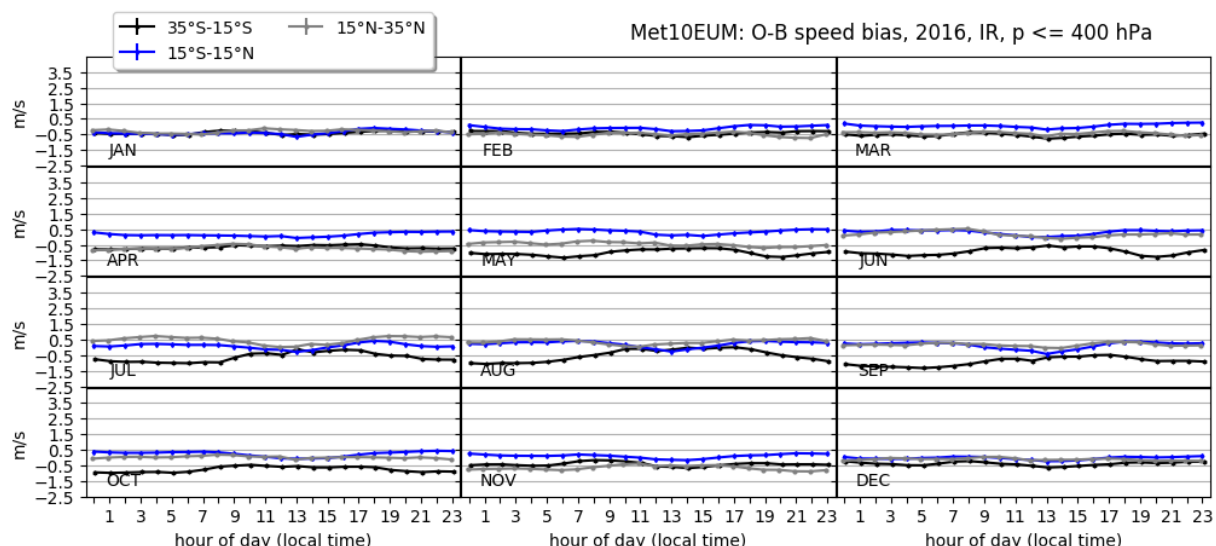
**Figure 4 : Pressure assigned to Met10EUM AMV ( $p_{AMV}$ ) vs collocated best-fit pressure ( $p_{best-fit}$ ). Differences  $p_{AMV} - p_{best-fit}$  are averaged for high-level winds ( $p \leq 400$  hPa) and over a  $2^\circ \times 2^\circ$  latitude x longitude grid.**

Figure 4 reveals that areas of large speed biases do not coincide with those areas exhibiting large differences between pressures assigned to Met10EUM AMVs ( $p_{AMV}$ ) and best-fit pressures ( $p_{best-fit}$ ). Typically,  $p_{AMV} - p_{best-fit}$  is less or equal 25 hPa. By contrast, for high-level winds, largest differences between AMV pressure and best-fit pressure are commonly found around the equator, where wind speed is  $< 20 \text{ ms}^{-1}$  and the O-B speed bias is less pronounced ( $< 2 \text{ ms}^{-1}$ ).

Observed speed biases may be linked to the growth and decay of convective cells. In the tropics, differences in the diurnal cycle of convection are apparent between oceans and land. While oceanic deep convection tends to reach its maximum in the early morning, convection over land reaches its maximum in the evening as a result of solar heating (Yang and Slingo, 2000). In a first step, we check if observed O-B speed biases are correlated with the diurnal cycle of convection. To this end, O-B speed biases for three different zonal bands are calculated and plotted against local daytime. Figure 5 shows mean wind speed differences between Met10EUM and ECMWF as function of local daytime for high-level winds. The absolute value of O-B speed bias is typically  $< 0.5 - 1 \text{ ms}^{-1}$ . A clear dependency

|   |  |              |
|---|--|--------------|
|  | <p align="center"><b>Study of AMV speed biases in the tropics</b></p> <p align="center"><b>Mid-term review report</b></p> <p align="center"><b>Results Task 1 - Task 3</b></p> |              |
| Reference: AMV-TN-0004-TS_Ed1_Rev1  | Date : 17/04/2019  | Page : 20/59 |

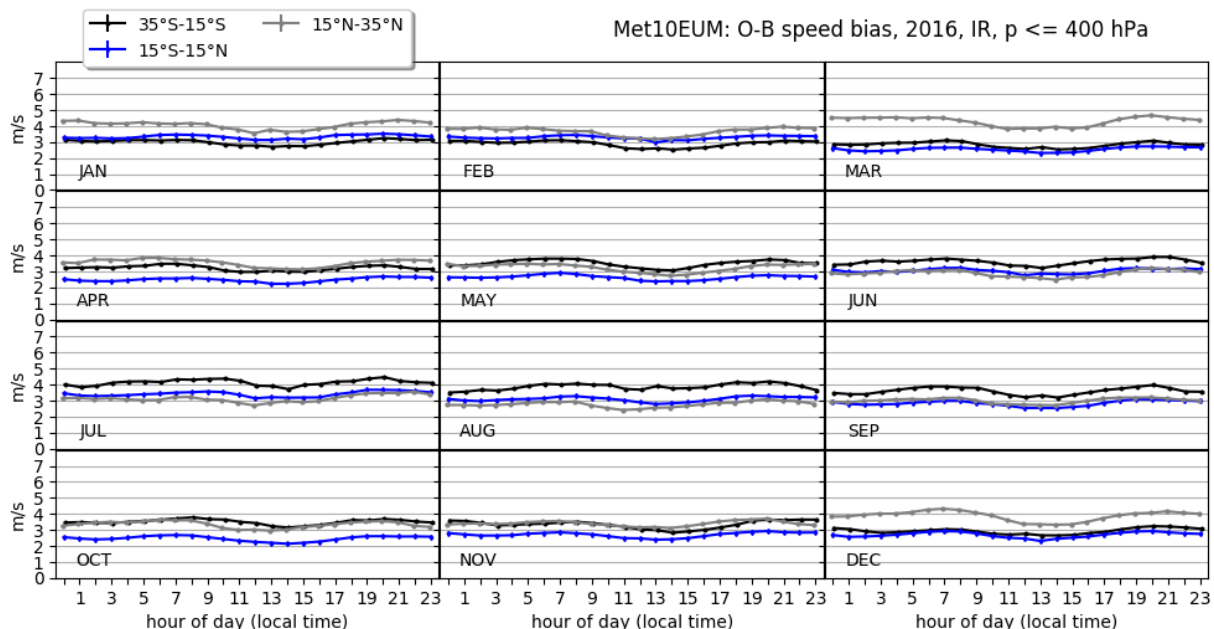
between bias and diurnal cycle of convection is not visible. Differences in O-B speed biases between different hours is typically  $< 0.5 \text{ ms}^{-1}$ . Only in July and August, differences of up to  $1.5 \text{ ms}^{-1}$  are obtained for the  $35^{\circ}\text{S}$ - $15^{\circ}\text{S}$  zonal band. Note the typical standard deviation of the mean speed differences exceeds the range of the ordinate in the plots (not shown in plots).



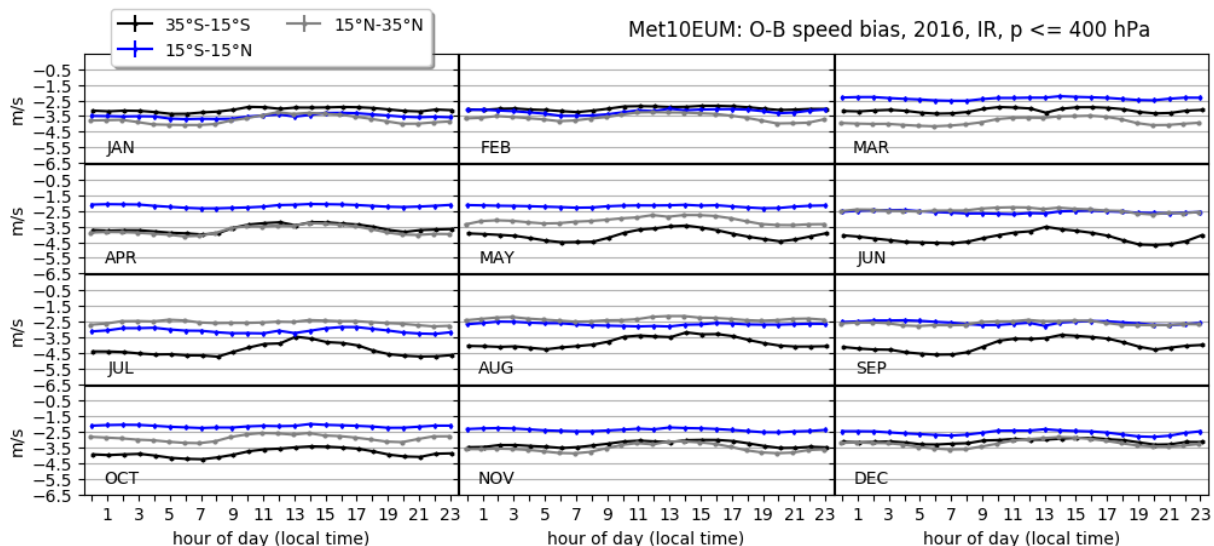
**Figure 5 : Diurnal cycle of Met10EUM O-B speed bias for three zonal bands ( $35^{\circ}\text{S}$ - $15^{\circ}\text{S}$ ,  $15^{\circ}\text{S}$ - $15^{\circ}\text{N}$ ,  $15^{\circ}\text{N}$ - $35^{\circ}\text{S}$ ) and high-level winds.**

Figure 5 shows that both positive and negative mean wind speed differences are present within one zonal band. By computing the O-B speed bias over such a zonal band, positive and negative biases may balance out, obscuring any diurnal variations of the speed bias. In Figure 6 and Figure 7, the diurnal cycle of the wind speed bias is plotted for positive differences and negative differences only, respectively. However, in both case no clear dependency of the speed bias with daytime is apparent. Speed biases vary only slightly with daytime; maximally by  $1 \text{ ms}^{-1}$ .






**Figure 6 :** As Figure 5, but only positive Met10EUM-ECMWF wind speed differences are used.

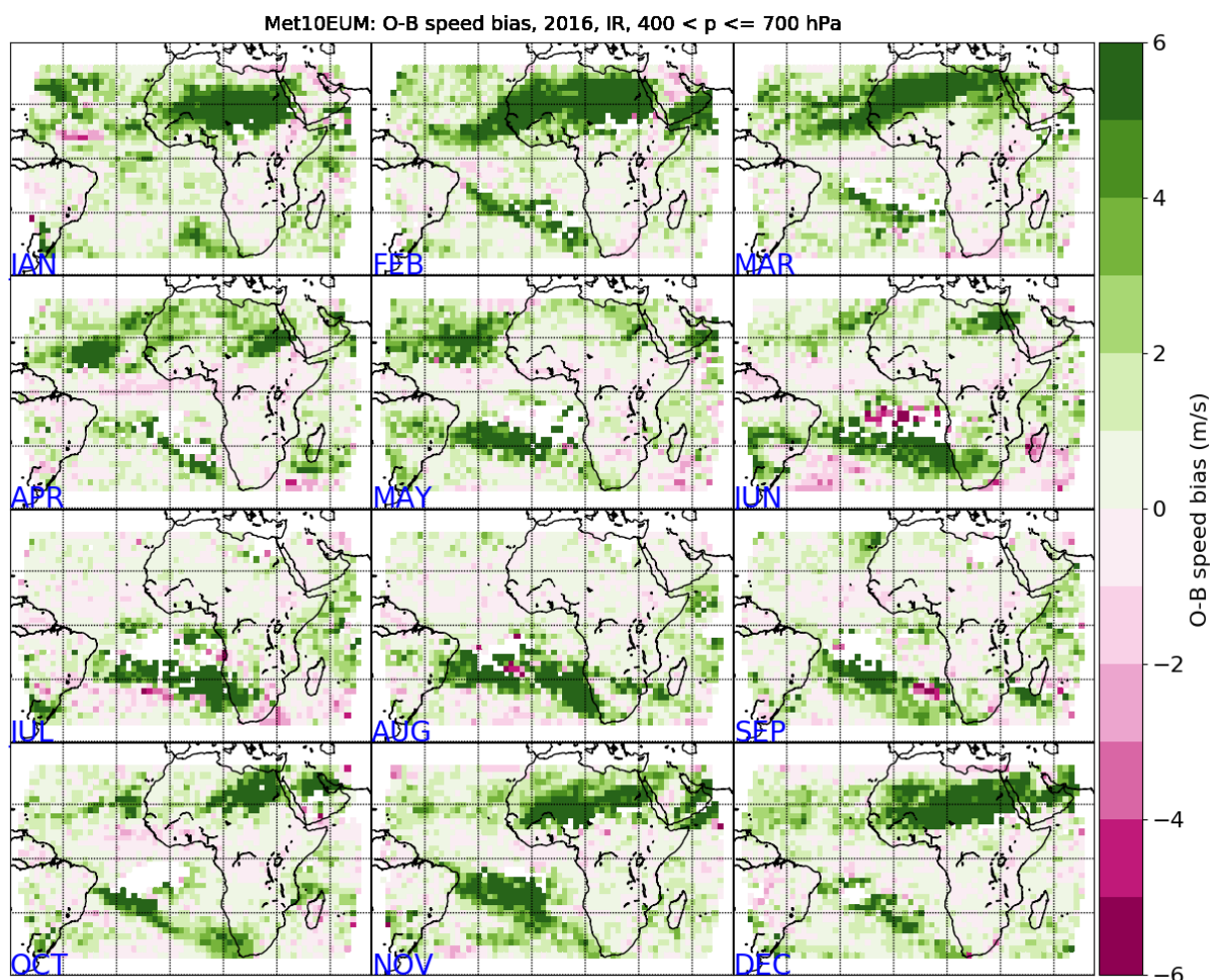


**Figure 7 :** As Figure 5, but only negative Met10EUM-ECMWF wind speed differences are used.

**Mid-level winds:** Figure 8 shows the spatial distribution of monthly mean differences between AMV Met10EUM and ECMWF for mid-level winds. Similar to high-level winds, differences  $> 6 \text{ ms}^{-1}$  are found over the Sahara desert in the northern hemisphere winter. Conversely, largest wind speed differences


|   |  |              |
|---|--|--------------|
|  | <p align="center"><b>Study of AMV speed biases in the tropics</b></p> <p align="center"><b>Mid-term review report</b></p> <p align="center"><b>Results Task 1 - Task 3</b></p> |              |
| Reference: AMV-TN-0004-TS_Ed1_Rev1  | Date : 17/04/2019  | Page : 22/59 |

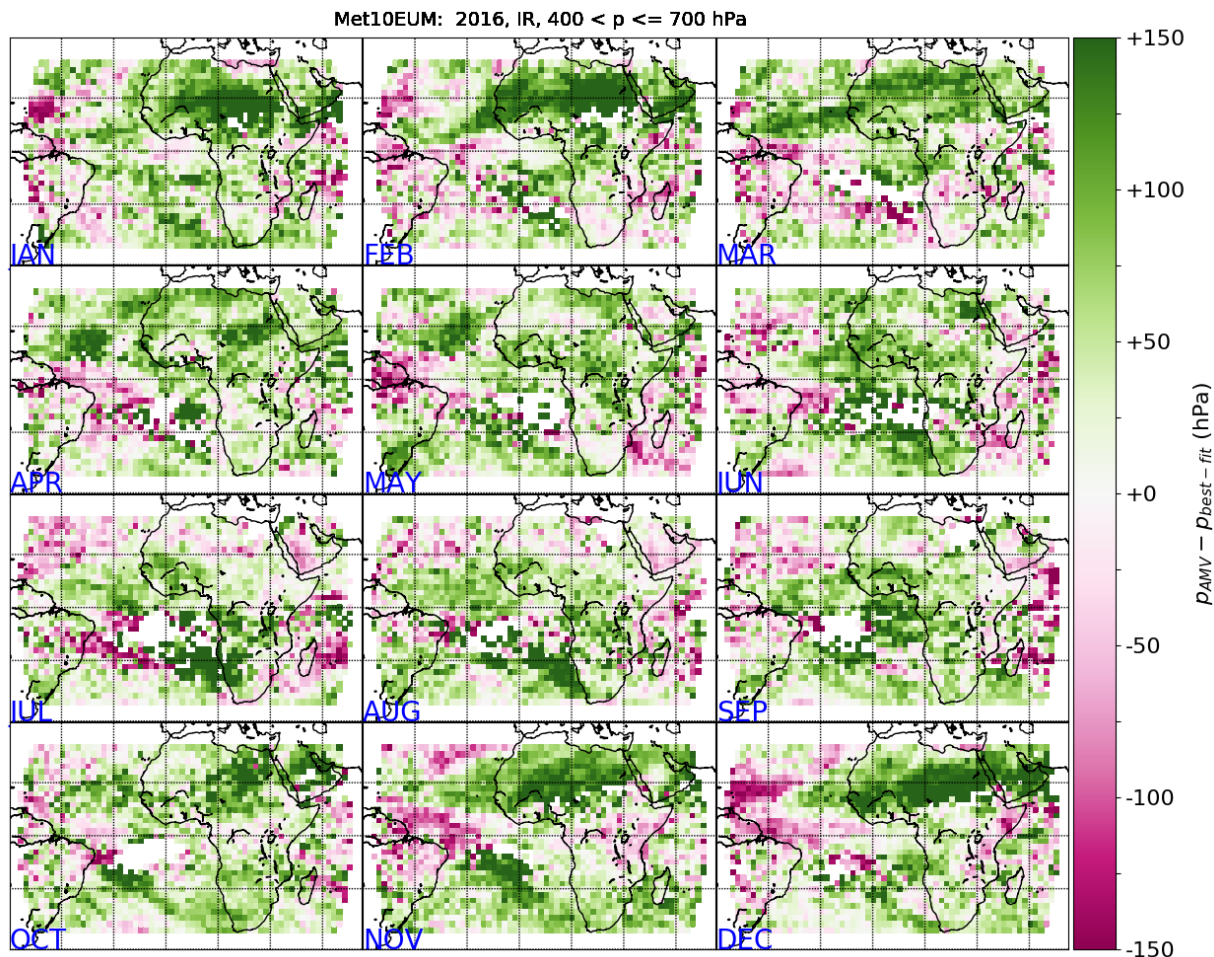
during southern hemisphere winter are obtained over the Atlantic Ocean, between Brazil and Namibia/South Africa.



**Figure 8 : As Figure 3, but for mid-level winds (400 hPa < p ≤ 700 hPa).**

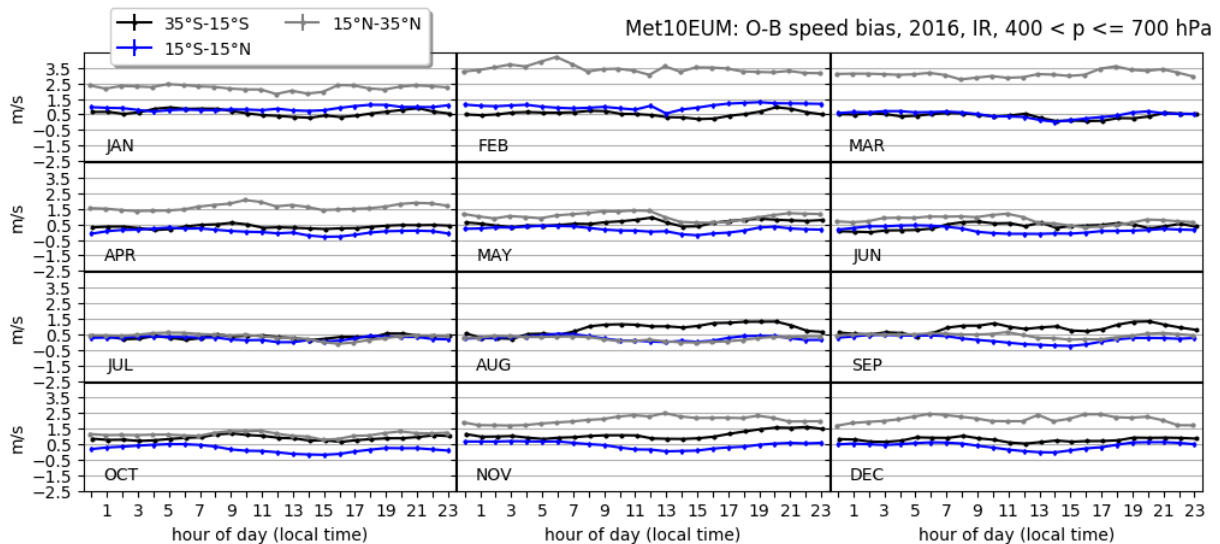
Figure 9 shows that mean differences between pressures assigned to AMV and the best-fit pressure are > 100 hPa over regions of exhibiting high wind speed discrepancies. Thus, AMVs are assigned to too low in the atmosphere and in conjunction with vertical wind shear lead to observed positive O-B speed bias greater than 6 ms<sup>-1</sup> at these locations.

|   |  |              |
|---|--|--------------|
|  | <p align="center"><b>Study of AMV speed biases in the tropics</b></p> <p align="center"><b>Mid-term review report</b></p> <p align="center"><b>Results Task 1 - Task 3</b></p> |              |
| Reference: AMV-TN-0004-TS_Ed1_Rev1  | Date : 17/04/2019  | Page : 23/59 |



**Figure 9 : Pressure assigned to Met10EUM AMV ( $p_{AMV}$ ) vs collocated best-fit pressure ( $p_{best-fit}$ ). As Fig. 4 but differences  $p_{AMV} - p_{best-fit}$  are averaged for mid-level winds ( $400 \text{ hPa} < p \leq 700 \text{ hPa}$ ).**

Mean wind speed differences between Met10EUM and ECMWF as function of local daytime for mid-level winds are displayed in Figure 10. Similar to high-level winds, no clear dependency of the bias on local daytime is apparent for any zonal band. Diurnal variations in speed bias are  $< 1 \text{ ms}^{-1}$ .



**Figure 10 : Diurnal cycle of Met10EUM O-B speed bias for three zonal bands (35°S-15°S, 15°S-15°N, 15°N-35°S) and mid-level winds.**

**Low-level winds:** The spatial distribution of monthly mean wind speed differences between low-level AMV Met10EUM and ECWMF is given in Figure 11. Wind speed differences are mostly  $\leq 1 \text{ ms}^{-1}$ , except for some arid locations in Northern Africa, where larger positive speed biases were found. Comparison to best-fit pressure reveals that AMVs are mostly assigned too low in the atmosphere (Figure 12). As the impact of the height assignment errors appears small, we can conclude that vertical wind shear was small at these altitudes.

Similar to high- and mid-level winds, the correlation between speed bias and diurnal cycle of convection was analysed (Fig. 13). As for high- and mid-level winds, variations of the speed bias during the day is small for the different zonal bands.



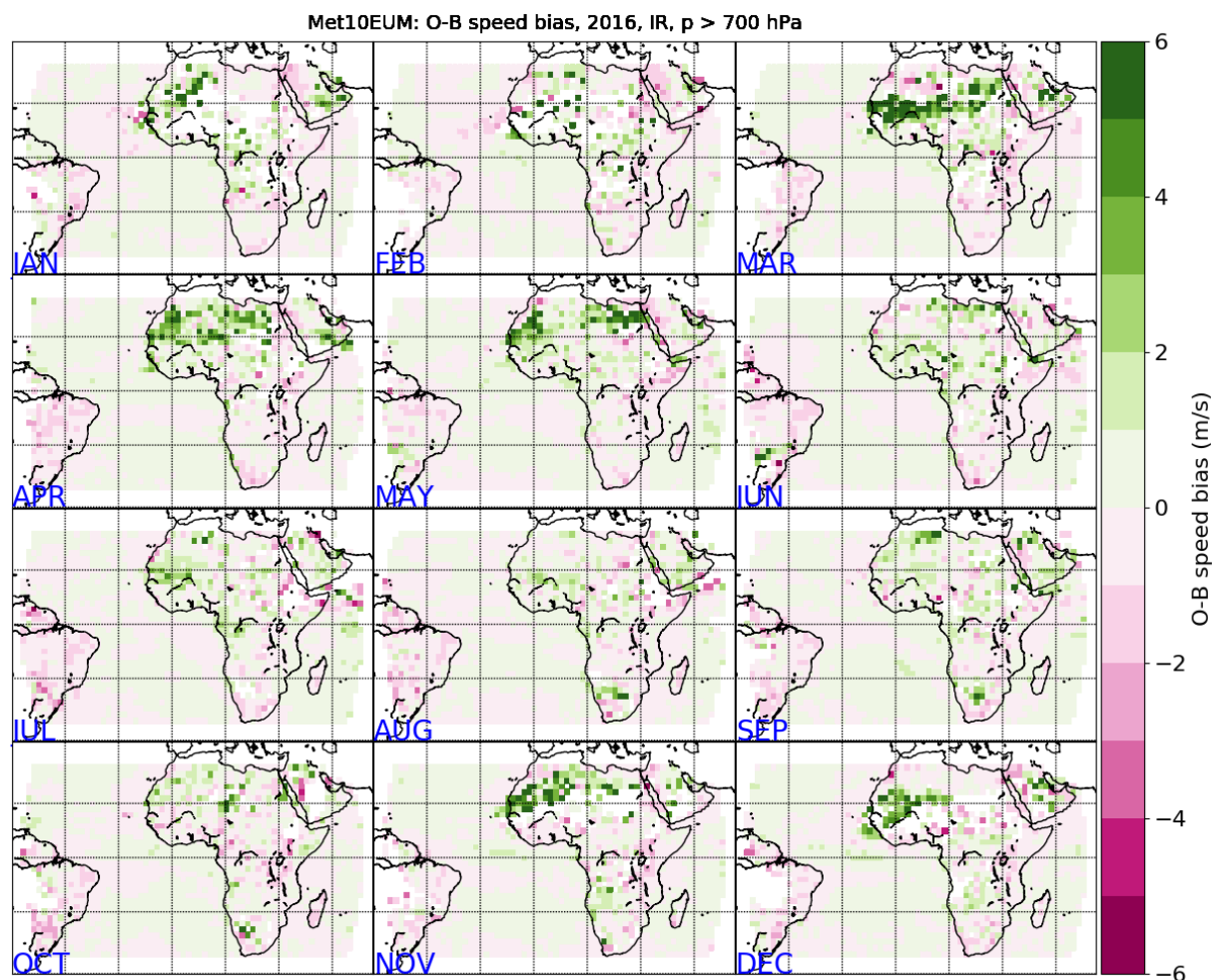

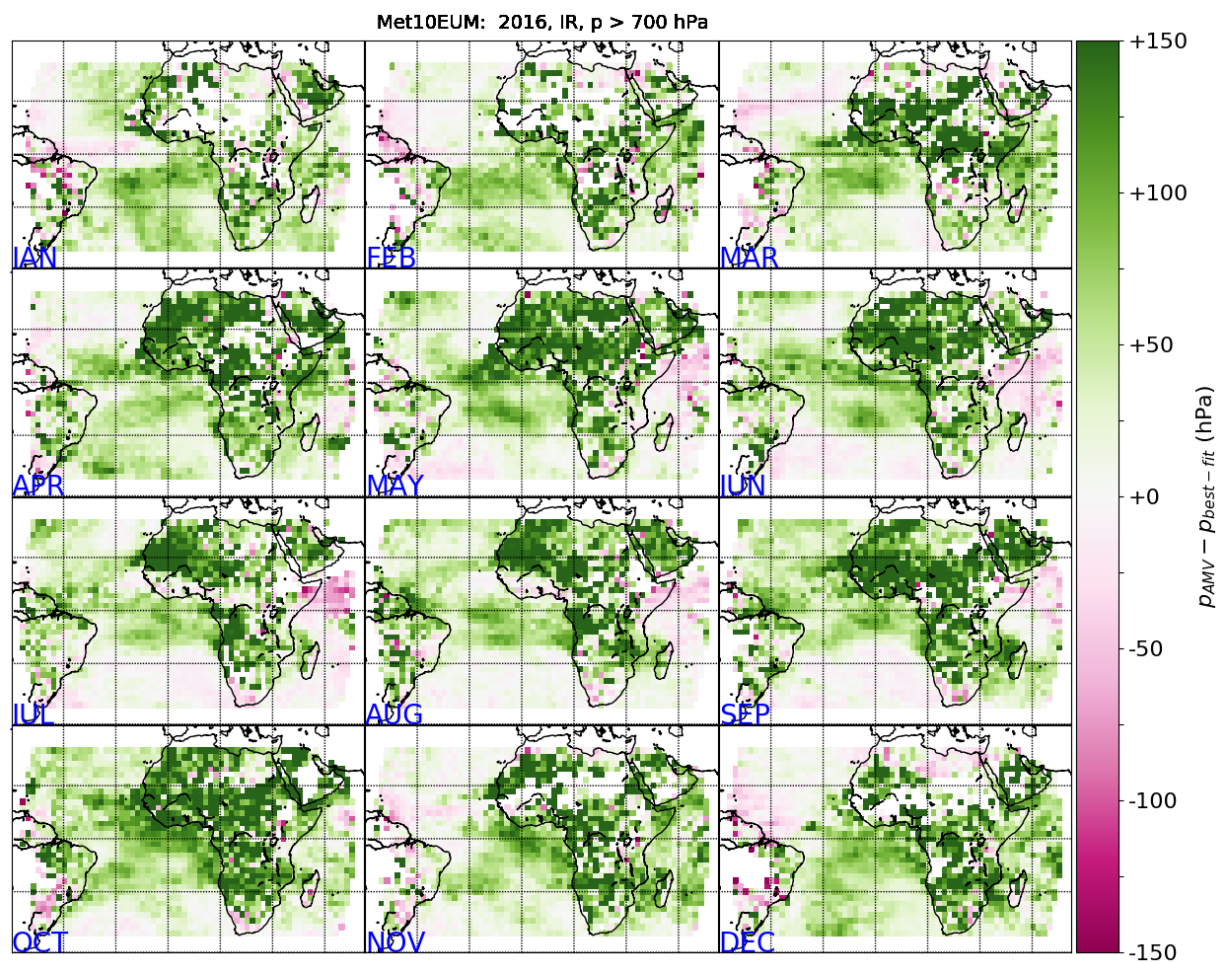
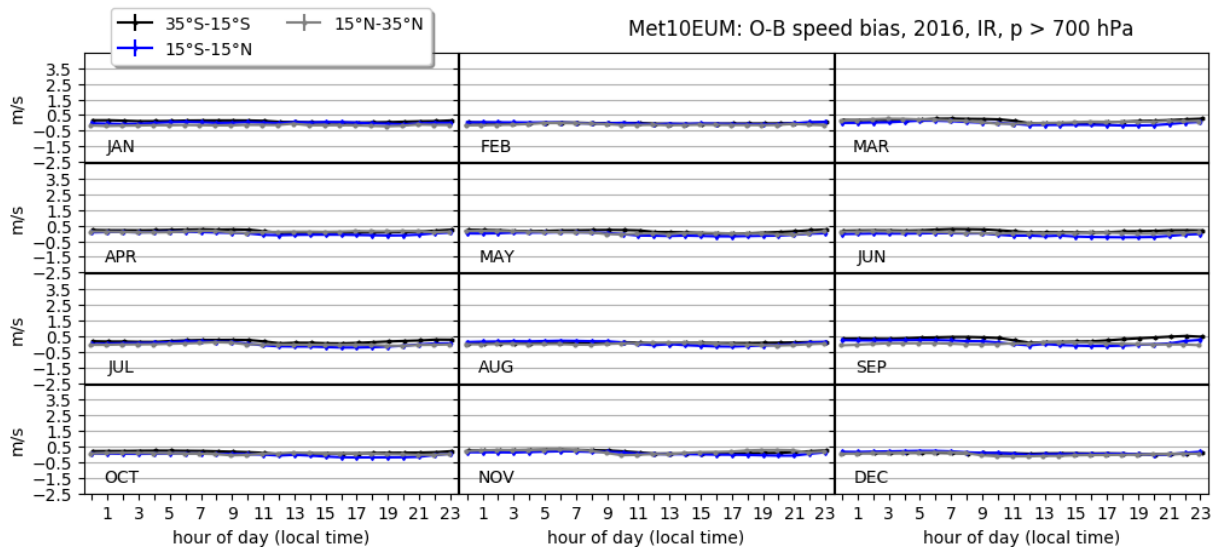


Figure 11 : As Figure 3, but for low-level winds ( $p > 700$  hPa).

|   |  |              |
|---|--|--------------|
|  | <p align="center"><b>Study of AMV speed biases in the tropics</b></p> <p align="center"><b>Mid-term review report</b></p> <p align="center"><b>Results Task 1 - Task 3</b></p> |              |
| Reference: AMV-TN-0004-TS_Ed1_Rev1  | Date : 17/04/2019  | Page : 26/59 |



**Figure 12 : Pressure assigned to Met10EUM AMV ( $p_{AMV}$ ) vs collocated best-fit pressure ( $p_{best-fit}$ ). As Figure 4, but differences  $p_{AMV} - p_{best-fit}$  are averaged for mid-level winds ( $p > 700$  hPa).**




**Figure 13 : Diurnal cycle of Met10EUM's O-B speed bias for three zonal bands (35°S-15°S, 15°S-15°N, 15°N-35°S) and low-level winds.**

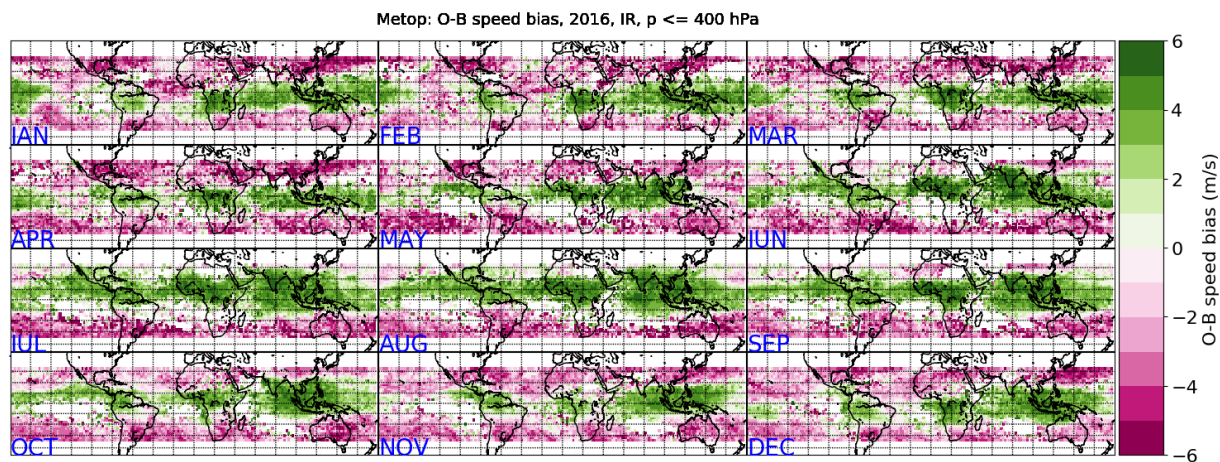
### 3.2.2 AMVs from Metop IR imagery

**High-level winds:** The geographic distribution of Metop AMV wind speed against collocated ECMWF wind speeds is given in Figure 14. Metop mostly reports higher wind speeds than ECMWF in the equatorial regions, where the average wind speed is typically below < 20 ms 1 (Figure 15). This positive O-B speed bias turns negative towards mid-latitudes, where wind speeds are higher.

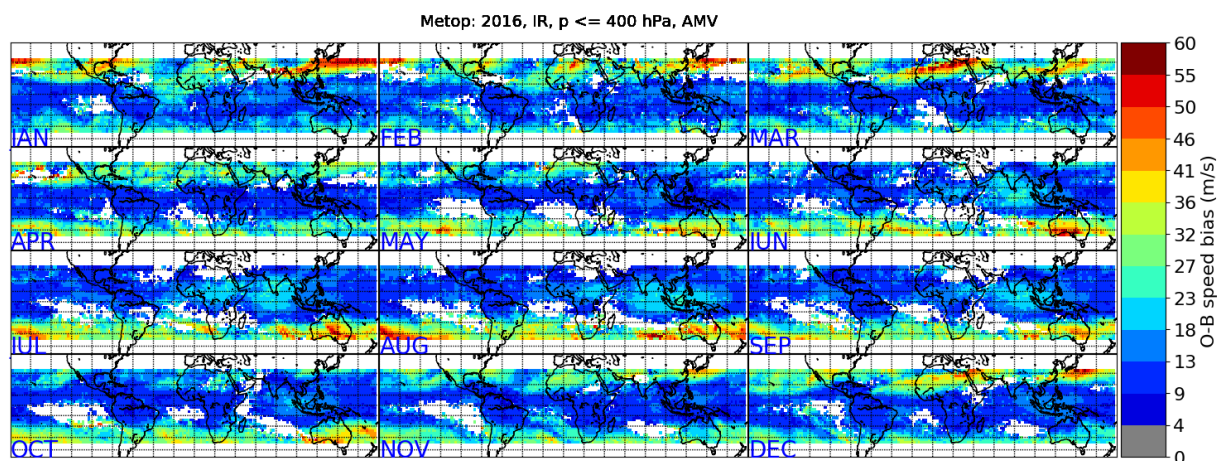
The  $p \leq \pm 25$  hPa vertical collocation criteria is relaxed to investigate height-assignment differences between ECWMF and Metop. Comparison of the spatial distribution of the speed bias (Fig. 14) to the spatial distribution of the best-fit pressure statistics (Figure 16) shows that over equatorial regions of South- and Central America and over Pacific regions,  $p_{\text{best-fit}}$  is mostly larger than  $p_{\text{AMV}}$ . Too high altitudes assigned to AMVs would lead to negative O-B speed biases, which, however, was not observed. For AMVs derived over the northern Indian Ocean in May to September,  $p_{\text{AMV}}$  are larger than  $p_{\text{best-fit}}$ , which may explain parts of the observed positive speed bias over these regions. For regions polewards of the equator, differences  $p_{\text{AMV}} - p_{\text{best-fit}}$  are typically smaller than 50 hPa and tend to be negative, indicating that AMVs are assigned too high altitudes.



|   |  |              |
|---|--|--------------|
|  | <p align="center"><b>Study of AMV speed biases in the tropics</b></p> <p align="center"><b>Mid-term review report</b></p> <p align="center"><b>Results Task 1 - Task 3</b></p> |              |
| Reference: AMV-TN-0004-TS_Ed1_Rev1  | Date : 17/04/2019  | Page : 28/59 |




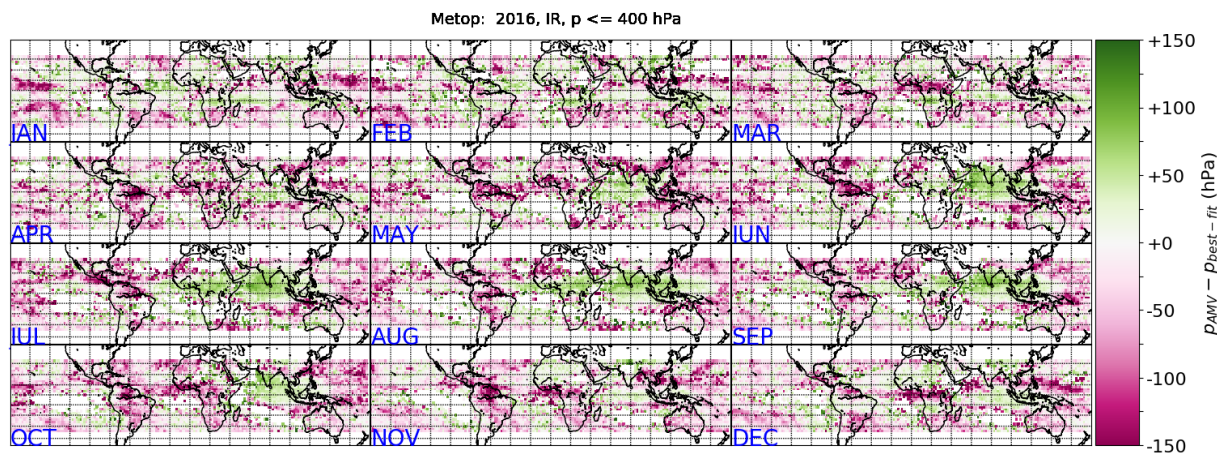
**Figure 14 : Geographic distribution of tropical Metop wind speed against collocated ECMWF winds. O-B bias is averaged for high levels ( $p \leq 400$  hPa) and over a  $2^\circ \times 2^\circ$  latitude x longitude grid.**



**Figure 15 : Geographic distribution of tropical Metop wind speeds averaged for high levels ( $p \leq 400$  hPa) and over a  $2^\circ \times 2^\circ$  latitude x longitude grid. Collocation criteria as described in Sec. 3.1 are used.**

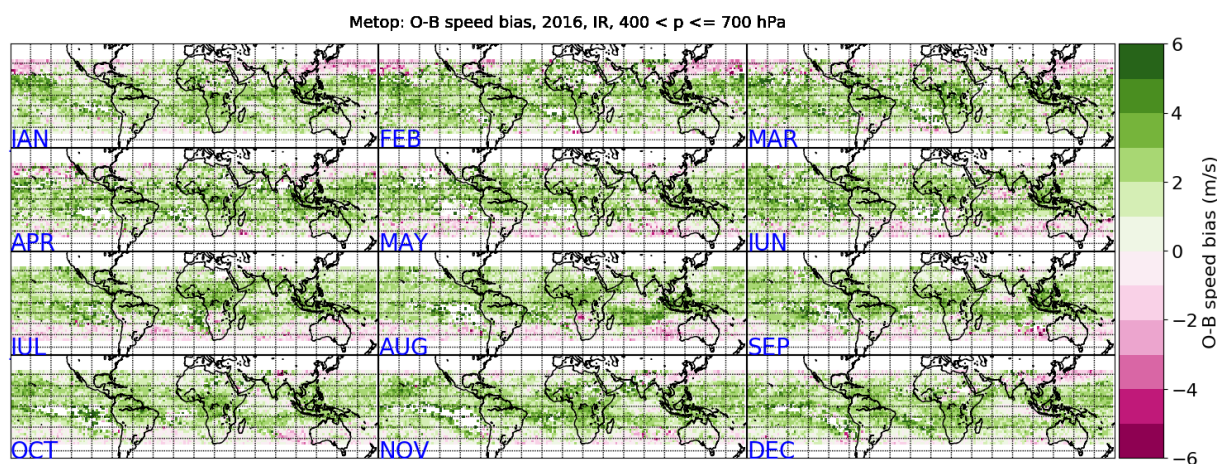


|   |  |              |
|---|--|--------------|
|  | <p align="center"><b>Study of AMV speed biases in the tropics</b></p> <p align="center"><b>Mid-term review report</b></p> <p align="center"><b>Results Task 1 - Task 3</b></p> |              |
| Reference: AMV-TN-0004-TS_Ed1_Rev1  | Date : 17/04/2019  | Page : 29/59 |




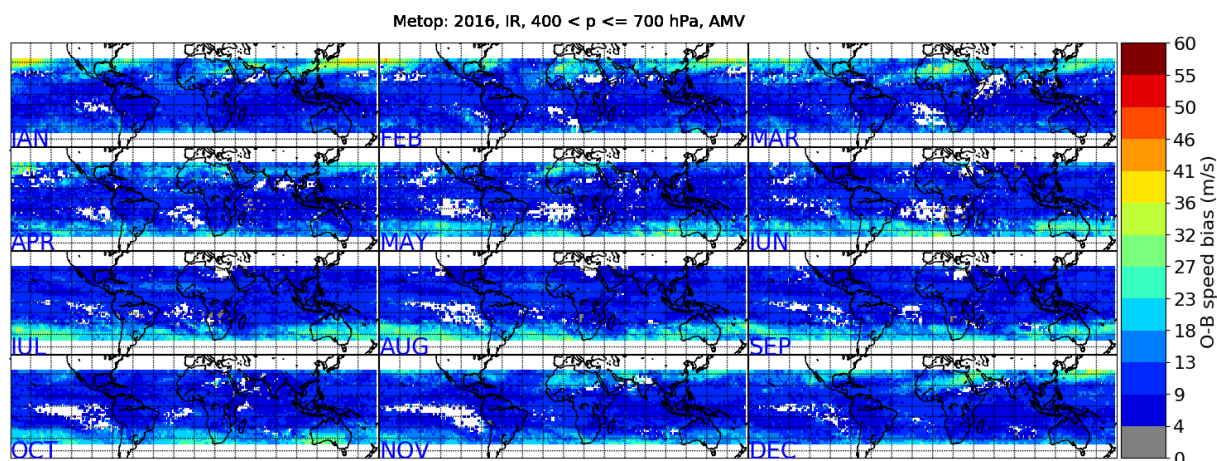
**Figure 16 : Pressure assigned to Metop AMV ( $p_{AMV}$ ) vs collocated best-fit pressure ( $p_{best-fit}$ ). Differences  $p_{AMV} - p_{best-fit}$  are averaged for high levels ( $p \leq 400$  hPa) and over a  $2^\circ \times 2^\circ$  lat x lon grid.**

**Mid-level winds:** Geographic distribution of the mean wind speed differences Metop-ECWMF are shown in Figure 17. Their spatial structure resembles that of high-level winds, that is, Metop report larger wind speeds than ECMWF for equatorial regions and tends to reports smaller wind speeds than ECMWF for latitudes that connect northern and southern to the equatorial region. The amplitude of reported mean differences is smaller than that reported for high-level winds, likely due to much smaller wind speed at these altitudes (Figure 18). Comparison of AMV pressure to best-fit pressure is given in Figure 19.  $p_{AMV} - p_{best-fit}$  is largest around the equator, with  $p_{AMV}$  being regularly 150 hPa larger than  $p_{best-fit}$ . Negative values of  $p_{AMV} - p_{best-fit}$  are mostly found over the Pacific.

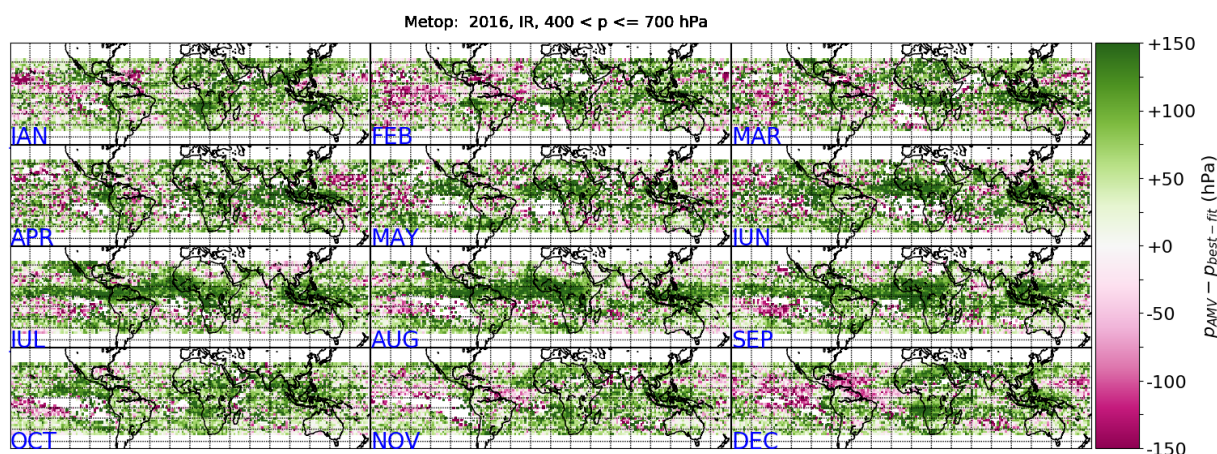


**Figure 17 : Geographic distribution of Metop wind speed against collocated ECMWF winds. O-B bias is averaged for mid-levels ( $400 \text{ hPa} < p \leq 700 \text{ hPa}$ ) and over a  $2^\circ \times 2^\circ$  latitude x longitude grid.**

|   |   |              |
|---|---|--------------|
|  | <p style="text-align: center;"><b>Study of AMV speed biases in the tropics</b></p> <p style="text-align: center;"><b>Mid-term review report</b></p> <p style="text-align: center;"><b>Results Task 1 - Task 3</b></p> |              |
| Reference: AMV-TN-0004-TS_Ed1_Rev1  | Date : 17/04/2019   | Page : 30/59 |




**Figure 18 : Geographic distribution of tropical Metop wind speeds averaged for mid levels (400 hPa <  $p \leq 700$  hPa) and over a  $2^\circ \times 2^\circ$  latitude x longitude grid. Collocation criteria as described in Sec. 3.1 are used.**

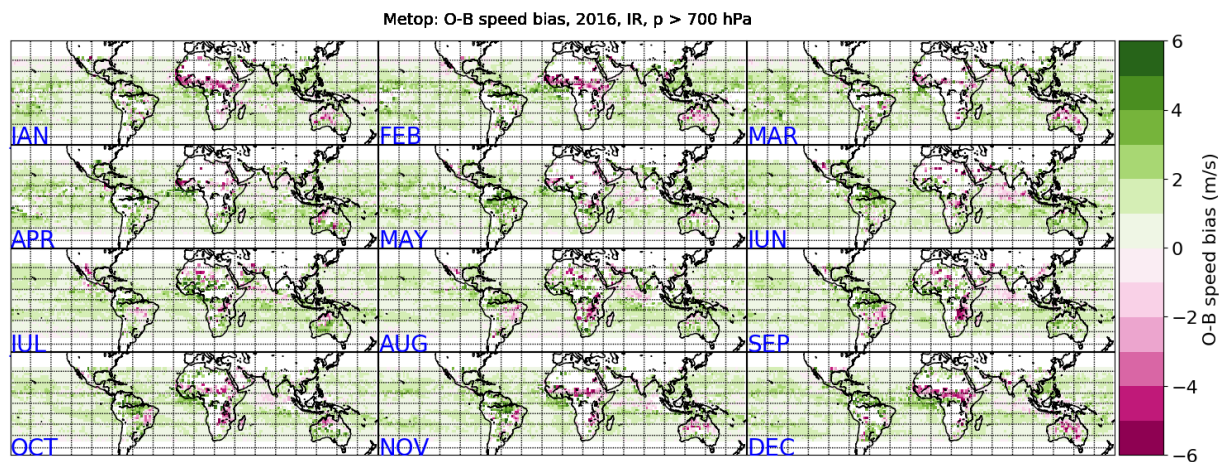


**Figure 19 : Pressure assigned to Metop AMV ( $p_{AMV}$ ) vs collocated best-fit pressure ( $p_{best-fit}$ ). Differences  $p_{AMV} - p_{best-fit}$  are averaged for mid-levels (400 hPa <  $p \leq 700$  hPa) and over a  $2^\circ \times 2^\circ$  latitude x longitude grid.**


**Low-level winds:** The O-B speed bias is mostly  $< 1 \text{ ms}^{-1}$  for low-level winds. Over the African continent, regions of larg O-B speed bias, up to  $-4 \text{ ms}^{-1}$  were obtained, e.g., from Senegal to Central Africa in Northern Hemisphere Winter (DJF), or over Southern Africa in August and September (Figure 20).



|   |  |              |
|---|--|--------------|
|  | <p align="center"><b>Study of AMV speed biases in the tropics</b></p> <p align="center"><b>Mid-term review report</b></p> <p align="center"><b>Results Task 1 - Task 3</b></p> |              |
| Reference: AMV-TN-0004-TS_Ed1_Rev1  | Date : 17/04/2019  | Page : 31/59 |



**Figure 20 : Geographic distribution of tropical Metop wind speed against collocated ECMWF winds. O-B bias is averaged for low levels ( $p > 700$  hPa) and over a  $2^\circ \times 2^\circ$  latitude x longitude grid.**

|   |  |              |
|---|--|--------------|
|  | <p align="center"><b>Study of AMV speed biases in the tropics</b></p> <p align="center"><b>Mid-term review report</b></p> <p align="center"><b>Results Task 1 - Task 3</b></p> |              |
| Reference: AMV-TN-0004-TS_Ed1_Rev1  | Date : 17/04/2019  | Page : 32/59 |

## 4 COMPARISON OF AMV TO REFERENCE OBSERVATIONS


### 4.1 MISR STEREO AMV

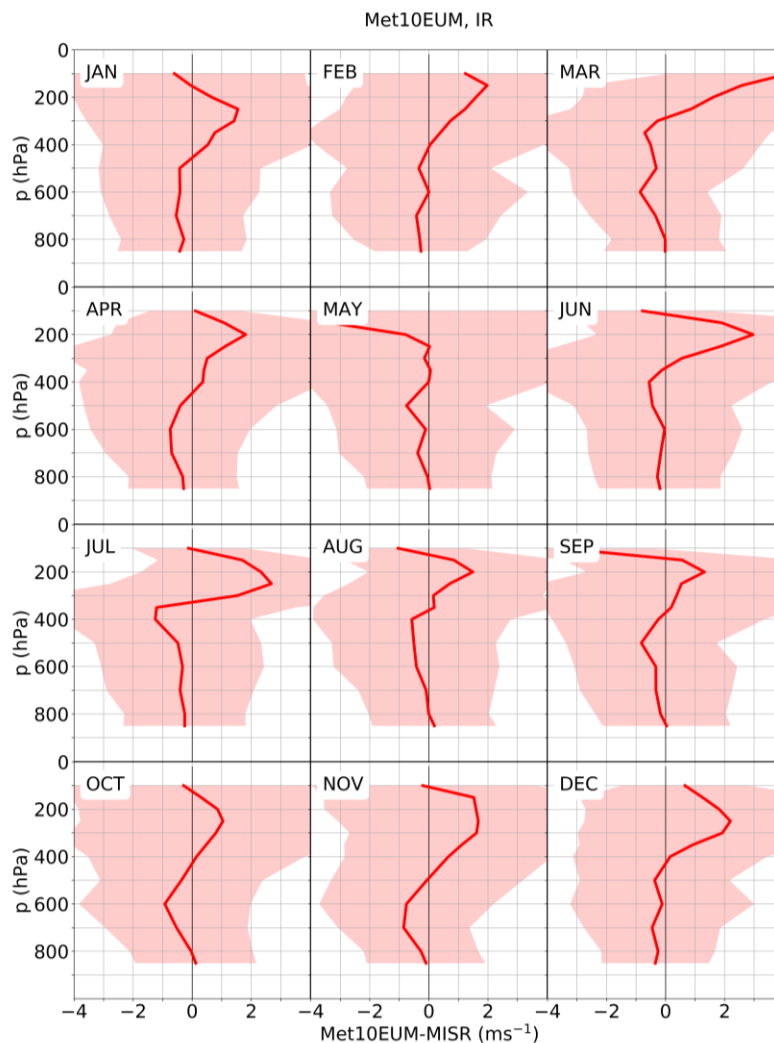
For comparison of Met10EUM and Metop AMVs to MISR stereo AMVs, the same collocation criteria as for the comparison to ECMWF winds are used. However, a horizontal collocation criteria needs to be introduced, i.e. MISR AMVs are compared to AMVs if data are within a horizontal distance of 150 km. If several MISR data meet the collocation criteria, the median then is calculated and compared to the corresponding AMV. MISR AMV retrieval is independent of a priori atmospheric and humidity forecasts and retrieves cloud height and motion simultaneously (Horvath and Davies, 2001). MISR provides wind speed and direction at geometric heights, which are converted to pressure levels using temperature and pressure levels of the spatially and temporally closest ECMWF grid cell. The same ECMWF dataset is used for altitude to pressure conversion as for wind comparison of Sec. 3.

Profiles of the mean differences between Met10EUM AMV and MISR wind speeds is given in Figure 21 for each month in 2016. For low-level to mid-level winds, MISR winds tends to be faster than that of Met10EUM, up to  $1 \text{ ms}^{-1}$ . Conversely, for high-level winds up to 200 hPa, Met10EUM winds tends to be  $1\text{-}2 \text{ ms}^{-1}$  faster than MISR, except for May, where MISR winds are faster than Met10EUM AMVs at all altitudes. Above 200 hPa, results vary strong among the different months as both faster MISR winds and faster Met10EUM AMV winds are reported. It is important to note here, that we have compared winds from IR imagery (Met10EUM) to winds derived from VIS imagery (MISR). Consequently, parts of the discrepancies may be explained by the fact that both sensors do not see the same cloud, which is particularly true for semi-transparent clouds.


Monthly mean profiles for Metop AMVs vs MISR wind speeds are given in Figure 22. Up to around 400 hPa ( $p > 400 \text{ hPa}$ ), Metop winds are typically  $0.5$  to  $1.0 \text{ ms}^{-1}$  faster than MISR winds. Above 400 hPa ( $p < 400 \text{ hPa}$ ), the spread between Metop AMV and MISR wind speeds increases with altitude, with Metop winds being up to  $> 4 \text{ ms}^{-1}$  faster than MISR at altitudes of  $< 200 \text{ hPa}$ . As for Met10EUM, obtained wind speed differences may be partly explained by different channels used by Metop and MISR.

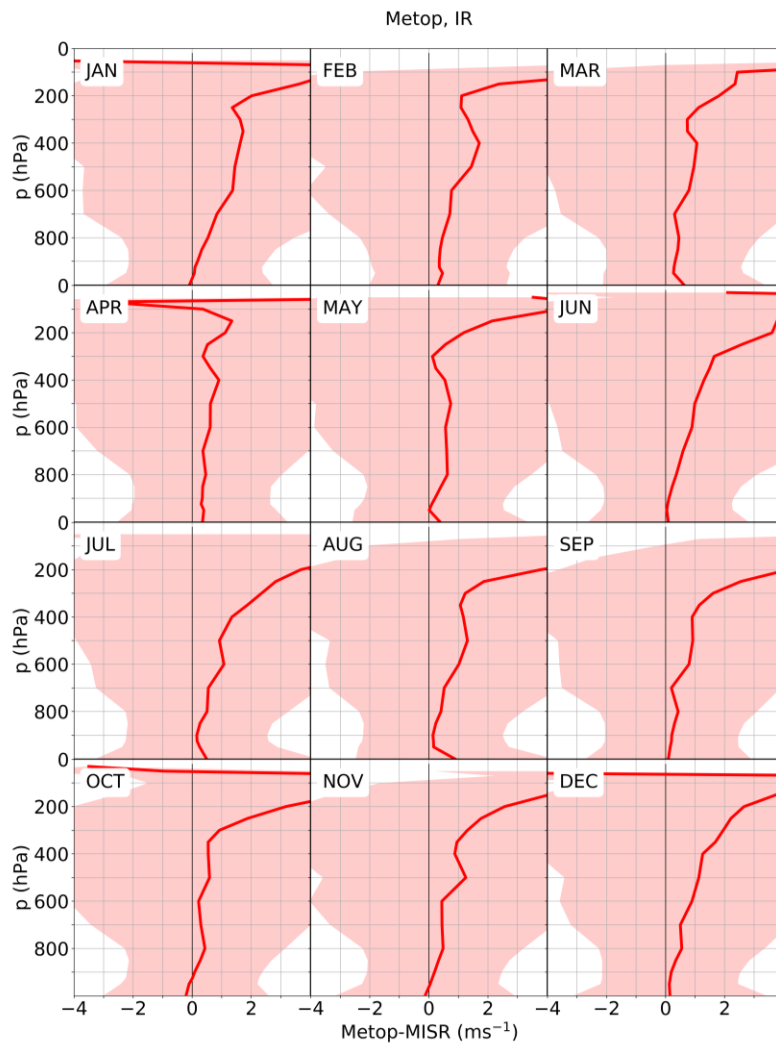
The geographic distribution of the mean Metop-MISR wind speed differences for high-level winds are given in Figure 23. Positive Metop-MISR wind speed differences larger than  $3 \text{ ms}^{-1}$  are frequently found over South-Eastern Asia and thus in a region where large mean Metop-ECMWF mean wind speed difference are found. Over southern oceans, Metop-MISR wind speed differences tend to be negative.

|   |   |              |
|---|---|--------------|
|  | <p style="text-align: center;"><b>Study of AMV speed biases in the tropics</b></p> <p style="text-align: center;"><b>Mid-term review report</b></p> <p style="text-align: center;"><b>Results Task 1 - Task 3</b></p> |              |
| Reference: AMV-TN-0004-TS_Ed1_Rev1  | Date : 17/04/2019   | Page : 33/59 |

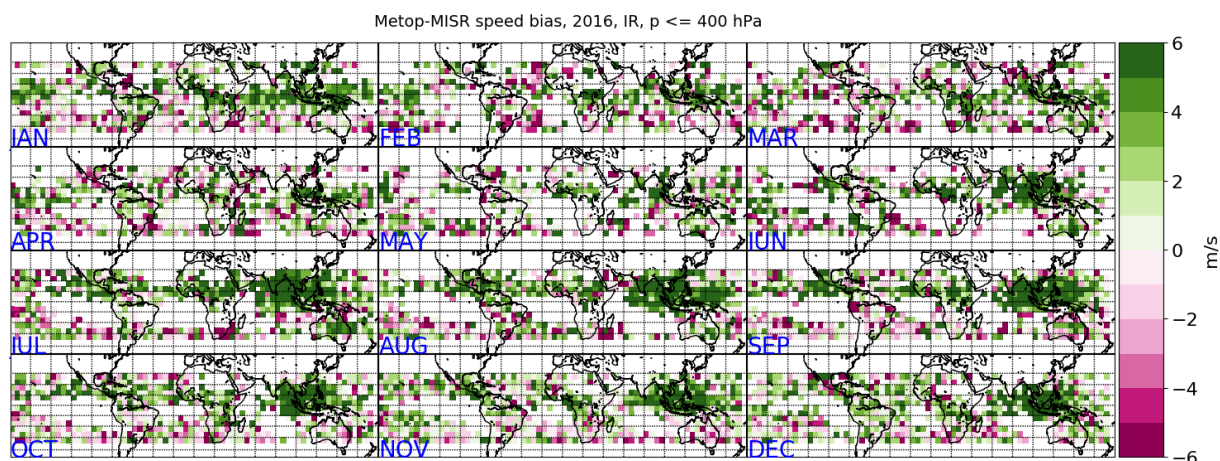


**Figure 21 : Monthly profiles of mean differences between Met10EUM AMV and MISR wind speeds (red line) and corresponding standard deviation (light red shades).**

|   |   |              |
|---|---|--------------|
|  | <p style="text-align: center;"><b>Study of AMV speed biases in the tropics</b></p> <p style="text-align: center;"><b>Mid-term review report</b></p> <p style="text-align: center;"><b>Results Task 1 - Task 3</b></p> |              |
| Reference: AMV-TN-0004-TS_Ed1_Rev1  | Date : 17/04/2019   | Page : 34/59 |



**Figure 22 : Monthly profiles of mean differences between Metop AMV and MISR wind speeds (red line) and corresponding standard deviation (light red shades).**



**Figure 23 : Geographic distribution of tropical Metop wind speeds against MISR winds averaged for high levels ( $p \leq 400$  hPa) and over a  $5^\circ \times 5^\circ$  latitude x longitude grid. Collocation criteria as described in Sec. 4.1 are used.**


## 4.2 RAOB WINDS

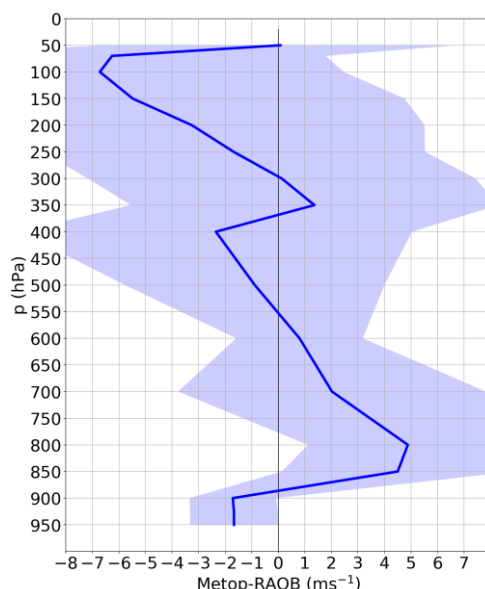
There are 2050 radiosondes observations (RAOB) available from IGRA in 2016 for latitudes  $\leq \pm 35^\circ$ . Table 3 provides an overview of RAOB data availability for different tropical regions. Most of the RAOB were obtained from ships located in Western Pacific, while no RAOB data were available over the Indian Ocean. The collocation criteria introduced in Sec. 4.1 were used to collocate RAOB with Met10EUM and Metop AMV, respectively. However, only matches with Metop were possible. Metop-RAOB matches were distributed irregularly over time. We only got matches in January, February, March, August and December, whereby only 1 match was available in January and only 7 matches in March. Due to this inhomogeneity, we did not attempt at grouping Metop-RAOB wind speed differences into months or different zonal bands.

**Table 3 : Overview RAOB data availability in tropics (latitudes  $\leq \pm 35^\circ$ ) for 2016. Number of radiosondes are grouped into Western Pacific ( $90^\circ\text{E} < \text{longitude} \leq 150^\circ\text{E}$ ), Indian Ocean ( $45^\circ\text{E} < \text{longitude} \leq 90^\circ\text{E}$ ) and Africa ( $-50^\circ\text{E} < \text{longitude} \leq 45^\circ\text{E}$ ).**

| Western Pacific | Indian Ocean | Africa | Other | Total |
|-----------------|--------------|--------|-------|-------|
| 865             | 0            | 588    | 597   | 2050  |

Figure 24 shows mean wind speed differences between Metop and RAOB as function of atmospheric pressure. In the lowermost troposphere ( $p \geq 900$  hPa) RAOB winds are  $2 \text{ ms}^{-1}$  faster than Metop. Above this altitude to about 600 hPa, Metop winds are faster than RAOB, up to  $5 \text{ ms}^{-1}$ . At 550 hPa, the differences change again sign, with RAOB reporting faster winds than Metop. This spread between Metop-RAOB mean wind speed differences then typically increases with increasing altitude. Note, a similar change of mean Metop-RAOB wind speed differences with altitude was also found by Horvath et al. (2017; their Fig. 5b), although they report smaller differences of  $< 2 \text{ ms}^{-1}$ .

|   |  |                     |
|---|--|---------------------|
|  | <b>Study of AMV speed biases in the tropics</b><br><br><b>Mid-term review report</b><br><br><b>Results Task 1 - Task 3</b> |                     |
| Reference: AMV-TN-0004-TS_Ed1_Rev1  | Date : 17/04/2019  | Page : <b>36/59</b> |



**Figure 24 : Profile of mean Metop-RAOB wind speed differences (blue) and corresponding standard deviation (blue shaded area). RAOB were collocated with Metop using criteria introduced in Sec. 3.**


### 4.3 CALIPSO CLOUD TOP HEIGHTS

Lidar cloud-top height observations from the polar-orbiting Cloud-Aerosol Lidar and Infrared Pathfinder Satellite Observations (CALIPSO) satellite are used to check the heights assigned to Met10EUM AMVs and investigate possible correlations between O-B speed bias and CALIPSO-AMV height differences. Initially, it was planned to compare CALIPSO cloud top heights also to Metop. However, no data met the collocation requirements described below. Additionally, no CALIPSO data were available for February 2016.

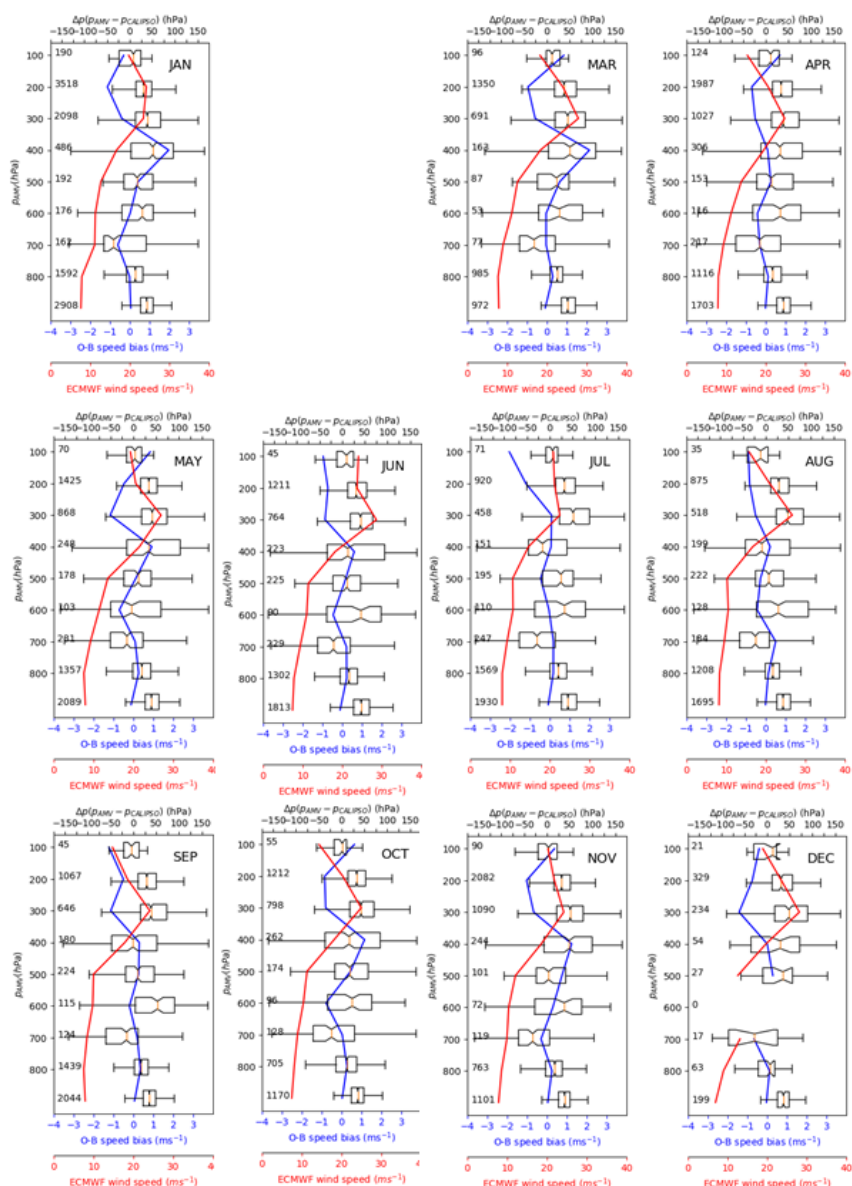
The applied collocation requirements have originally been developed by Folger and Weissmann (2014) and Weissmann et al. (2013) and were slightly modified for this task. Firstly, CALIPSO data are collocated with nearby AMVs if they are within a horizontal distance of 75 km and within 45 minutes of the location and time of each AMV. Secondly, the median value of all available (at least 20) individual CALIPSO cloud-top observations meeting the collocation criteria is taken and considered as representative cloud top. In addition, the root-mean-square differences between single lidar cloud observations and their median value must not exceed 100 hPa. We discarded all multilayer cloud observations and ensured that the detected lidar signal definitely represents a cloud. For the latter, this can be ensured by forcing the CALIPSO QI to exceed a value of 90. Finally, the AMVs must be within 165 hPa of the CALIPSO cloud top height.

Figure 25 reports the comparison of CALIPSO cloud top heights ( $p_{\text{CALIPSO}}$ ) with Met10EUM AMV pressures ( $p_{\text{AMV}}$ ). Only data are used where AMVs are collocated with ECMWF wind fields. Most collocations are found for 300, 400, 800 and 900 hPa levels. Overall,  $p$ , the median difference between collocated  $p_{\text{AMV}}$  and  $p_{\text{CALIPSO}}$ , is  $> 0$  hPa throughout the atmospheric profile (except for 700 hPa, where  $p$  is typically  $< 0$ ), which in turn means that AMVs tend to have assigned too low altitudes. Highest median




|   |   |              |
|---|---|--------------|
|  | <p style="text-align: center;"><b>Study of AMV speed biases in the tropics</b></p> <p style="text-align: center;"><b>Mid-term review report</b></p> <p style="text-align: center;"><b>Results Task 1 - Task 3</b></p> |              |
| Reference: AMV-TN-0004-TS_Ed1_Rev1  | Date : 17/04/2019   | Page : 37/59 |

pressure difference of 25 - 50 hPa are typically obtained between 300 and 400 hPa altitude and at 600 hPa altitude. At the 400 hPa layer, this peak in  $p$  often coincides with largest O-B speed bias of up to 2  $\text{ms}^{-1}$  (e.g. January, March, October, November). For these periods, highest wind speed is typically found around 300 hPa. As AMVs around 400 hPa have assigned too low altitudes, parts of the O-B speed bias obtained at these altitudes may be attributed to an average 30 hPa incorrect height assignment in conjunction with high wind speeds above 400 hPa. Interestingly, despite positive median values of  $p$ , O-B speed biases above 400 hPa ( $p < 400$  hPa) tend to be negative, i.e. ECMWF winds are faster than Met10EUM AMVs for the presented data.



**Figure 25 : Comparison of CALIPSO cloud top height with Met10EUM AMVs. Box-and-whisker plots of AMV-CALIPSO pressure ( $p_{\text{AMV}} - p_{\text{CALIPSO}}$ ) difference are shown for different AMV pressure**

|   |  |              |
|---|--|--------------|
|  | <p align="center"><b>Study of AMV speed biases in the tropics</b></p> <p align="center"><b>Mid-term review report</b></p> <p align="center"><b>Results Task 1 - Task 3</b></p> |              |
| Reference: AMV-TN-0004-TS_Ed1_Rev1  | Date : 17/04/2019  | Page : 38/59 |

levels, whereby each box contains data in a pressure range of 50 hPa. Each box extends from the lower to upper quartile values of the pressure differences, with a red line at the median. Corresponding O-B speed bias is shown in blue, while corresponding ECMWF speeds are shown in red. Numbers in the left part of each figure denote the number of collocations used to calculate pressure differences. No CALIPSO data were available for February 2016.

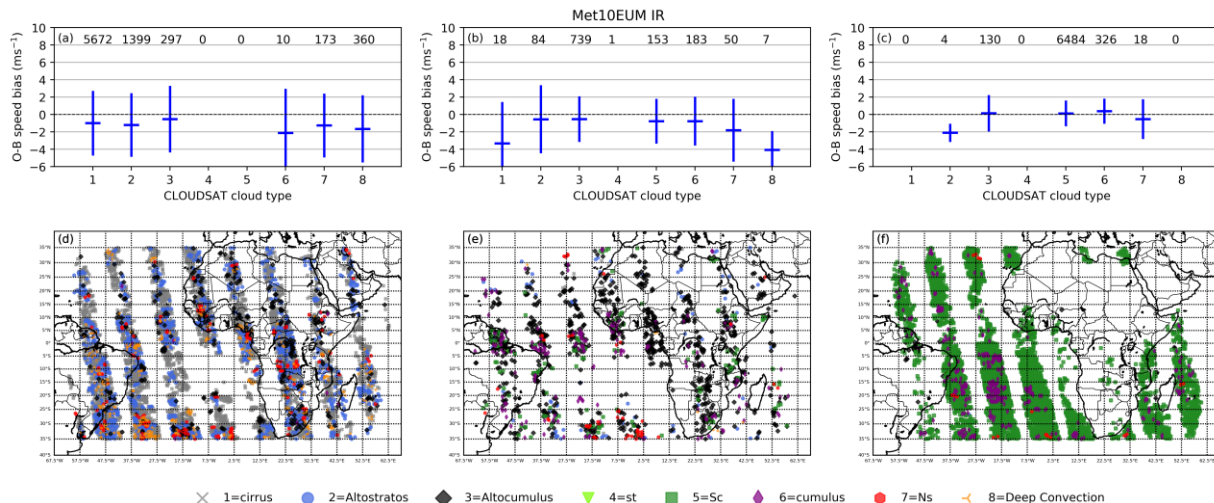
## 4.4 CLOUDSAT CLOUD TYPE CLASSIFICATION

Cloud type classification obtained from CLOUDSAT are used to investigate any correlation between cloud type and observed O-B speed bias. Based on the collocation database established in Sec. 3, we collocated any Met10EUM AMV with CLOUDSAT if horizontal, vertical and temporal distance are less than 150 km, less than 25 hPa and less than 30 minutes, respectively. In case several CLOUDSAT profiles meet the collocation criteria, we use the cloud top that is spatially closest to the Met10EUM AMV. CLOUDSAT cloud tops are reported on geometric heights. Similar to MISR stereo AMVs temperature and pressure from the spatially and temporally closest ECMWF grid cell are used to convert geometric heights to pressure.

Collocated O-B speed bias (Met10EUM AMV - ECMWF) as function of CLOUDSAT cloud type is given in Figure 26 for high-level, mid-level and low-level winds. At high-levels (Figure 26a), most collocated clouds are cirrus clouds, followed by Altostratus clouds. As expected, no stratus or stratocumulus cloud have been identified or matched at these altitudes. The O-B speed bias is relative similar for cirrus and altostratus clouds and around  $-1.5 \text{ ms}^{-1}$  (ECMWF faster than Met10EUM AMV), indicating no clear dependency of collocated speed bias and cloud type at these levels. Note, we separated results for different zonal bands ( $35^{\circ}\text{S}$ - $15^{\circ}\text{S}$ ,  $15^{\circ}\text{S}$ - $15^{\circ}\text{N}$ ,  $15^{\circ}\text{N}$ - $35^{\circ}\text{N}$ ) but no significant change with respect to results presented in Fig. 27a were found (plots not shown).

At mid-level, most clouds that could be collocated with Met10EUM AMVs were identified as altocumulus, cumulus and stratocumulus clouds (Figure 26b). As for high levels, there is no clear correlation between cloud type and collocated O-B speed bias, which is on average  $< 1.5 \text{ ms}^{-1}$  (ECMWF faster than Met10EUM AMV) for these three cloud types. As for high levels, results were separated for three different zonal bands but no significant change with respect to the results presented in Figure 26b were found.

At low levels, clouds are predominately of stratocumulus, while a small portion is classified as cumulus and altocumulus. For these three cloud types, collocated O-B speed bias is around  $< 0 \text{ ms}^{-1}$ .




**Figure 26 : Correlation of CLOUDSAT cloud types with observed O-B speed bias of Met10EUM AMVs against ECMWF winds for (a) high-level clouds, (b) mid-level and (c) low-level clouds. Horizontal blue lines denote mean wind speed differences Met10EUM AMV - ECMWF, while vertical blue lines denote the corresponding standard deviation. CLOUDSAT groups clouds into cirrus (1), altostratus (2), altostratus (3), stratus (4), stratocumulus (5), cumulus (6, including cumulus congestus), nimbostratus (7) and deep convection (8). Depicted are also geographical distribution of CLOUDSAT and Met10EUM AMV collocations for (d) high-level clouds, (e) mid-level and (f) low-level clouds. Results for 8 months averages are presented (January to August).**

## 4.5 OLR

### 4.5.1 Accumulated OLR from ECMWF

It is aimed to relate O-B speed bias to convective regimes to check whether different and strength of convection lead to weak/large O-B speed biases. OLR is commonly used to describe the general structure and depth of tropical convection. For instance, convective regions covered by cold tops typically appear as OLR minima ( $OLR < 260 \text{ Wm}^{-2}$ ). In this Section OLR from ECMWF are used to check the correlation between OLR and speed bias. At ECMWF, radiation parameters at single levels are so-called accumulated parameters, that is, the data is accumulated over certain time period. The units are Joule per square metre. Conversion to  $\text{Wm}^{-2}$  requires the accumulated values to be divided by the time period over which the data has been accumulated. For example, for a forecast step of 4 hours, the OLR in  $\text{Wm}^{-2}$  is calculated from the OLR in  $\text{Jm}^{-2}$  divided by  $4 \times 3600$  seconds. As we do not want to compare OLRs accumulated over different time steps, one time step is selected for the comparison.

Figure 27 compares ECMWF's OLR from forecast step 1 (that is, for 1 and 13 UTC) to the O-B speed bias obtained in Sec. 3. For all months, the OLR profile is very similar. OLR decreases with altitude as the blocking of long-wave radiation penetrating through clouds and cloud albedo increases with altitude. Above 600 hPa ( $p < 600 \text{ hPa}$ ), the medians of OLR are typically below  $260 \text{ Wm}^{-2}$ . The vertical profile of collocated O-B speed bias does not follow the vertical profile of OLR, indicating low correlation between convection and O-B speed bias.

|   |  |                     |
|---|--|---------------------|
|  | <p align="center"><b>Study of AMV speed biases in the tropics</b></p> <p align="center"><b>Mid-term review report</b></p> <p align="center"><b>Results Task 1 - Task 3</b></p> |                     |
| Reference: AMV-TN-0004-TS_Ed1_Rev1  | Date : 17/04/2019  | Page : <b>40/59</b> |

Results for Metop-EMWF speed differences vs OLR are given in Figure 28. Compared to Met10EUM, collocated OLR decreases stronger with altitude. In addition, OLR values are 20 - 50  $\text{Wm}^{-2}$  lower than those obtained for Met10EUM above 400 hPa ( $p < 400$  hPa), indicating that Metop is sensing in stronger convective regimes than Met10EUM at these altitudes. OLR minima above 200 hPa ( $p < 200$  hPa) coincide with maxima in O-B speed biases of  $> 2 \text{ ms}^{-1}$ . As for Met10EUM, the vertical profile of collocated O-B speed bias does not follow the vertical profile of OLR, indicating low correlation between convection and O-B speed bias.

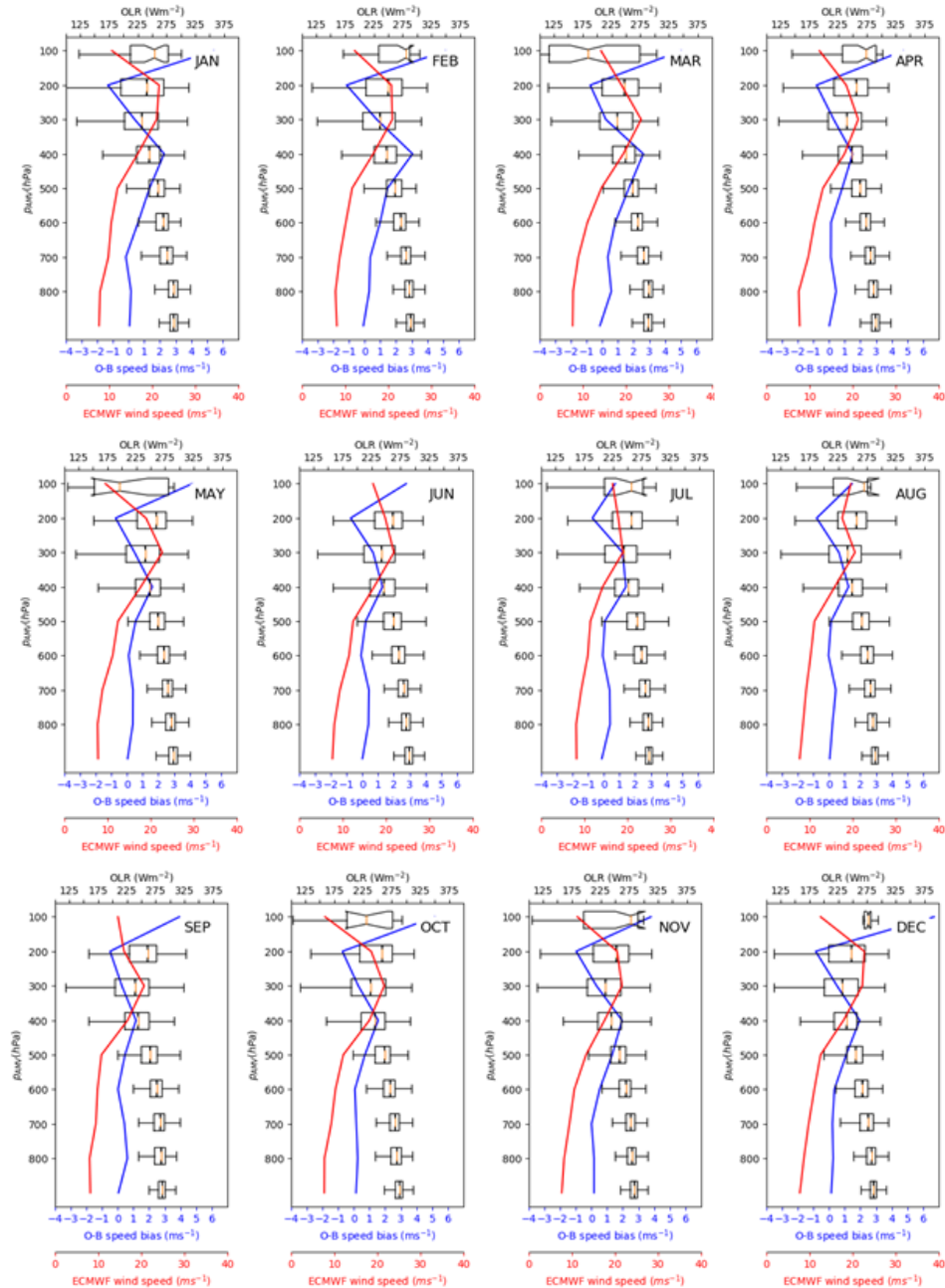

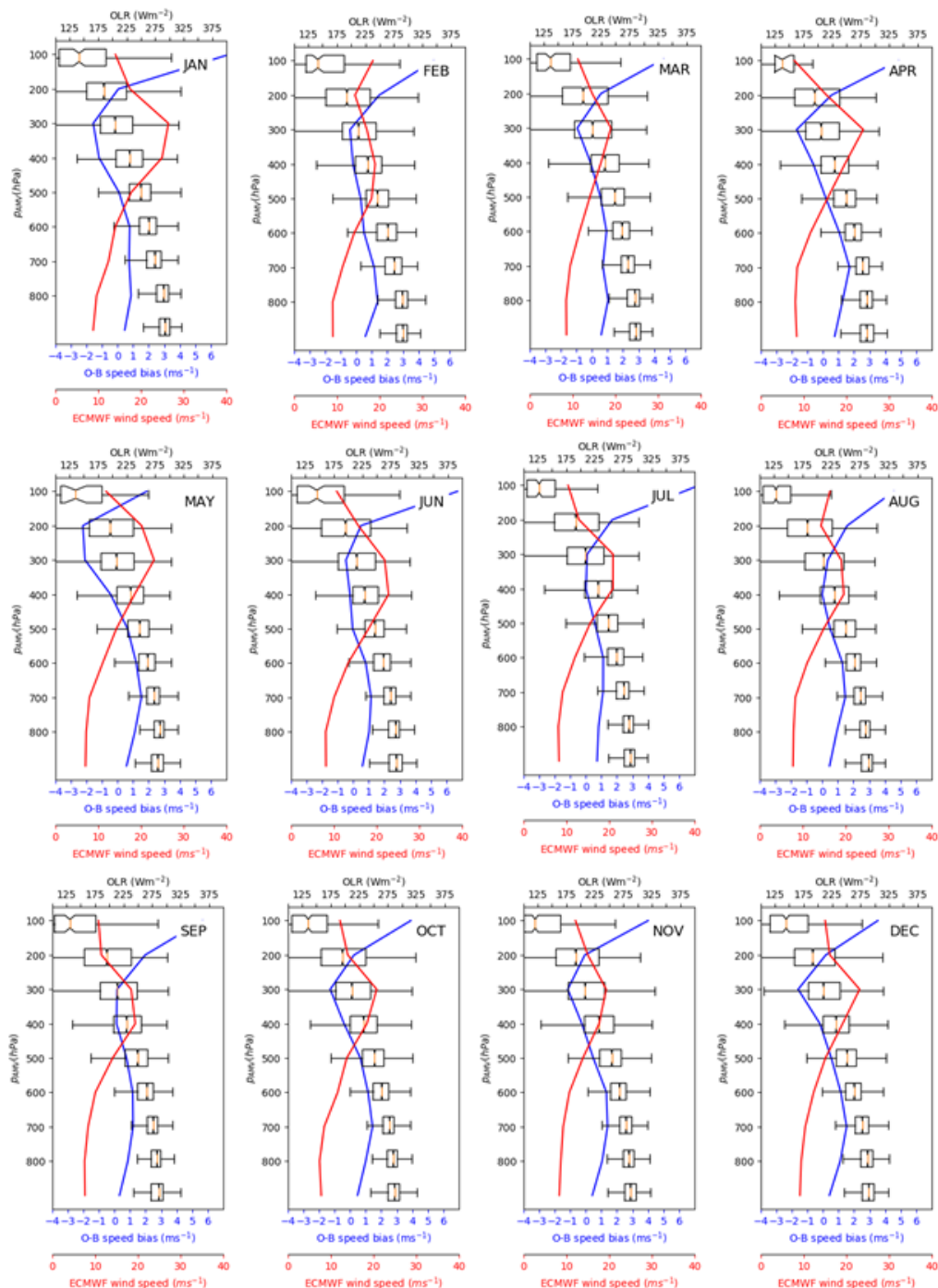



Figure 27 : Comparison of ECMWF OLR (step range = 1, see text) with Met10EUM AMVs. Box-and-whisker plots of OLR are shown for different AMV pressure levels. Each box extends from the lower to upper quartile values of the pressure differences, with a line at the median. Corresponding O-B speed bias is shown in blue, while ECMWF speeds are shown in red.

|   |  |              |
|---|--|--------------|
|  | <p align="center"><b>Study of AMV speed biases in the tropics</b></p> <p align="center"><b>Mid-term review report</b></p> <p align="center"><b>Results Task 1 - Task 3</b></p> |              |
| Reference: AMV-TN-0004-TS_Ed1_Rev1  | Date : 17/04/2019  | Page : 42/59 |



**Figure 28 : As Figure 27, but for Metop AMVs.**

|   |  |                     |
|---|--|---------------------|
|  | <p align="center"><b>Study of AMV speed biases in the tropics</b></p> <p align="center"><b>Mid-term review report</b></p> <p align="center"><b>Results Task 1 - Task 3</b></p> |                     |
| Reference: AMV-TN-0004-TS_Ed1_Rev1  | Date : 17/04/2019  | Page : <b>43/59</b> |


#### **4.5.2 OLR from AIRS**

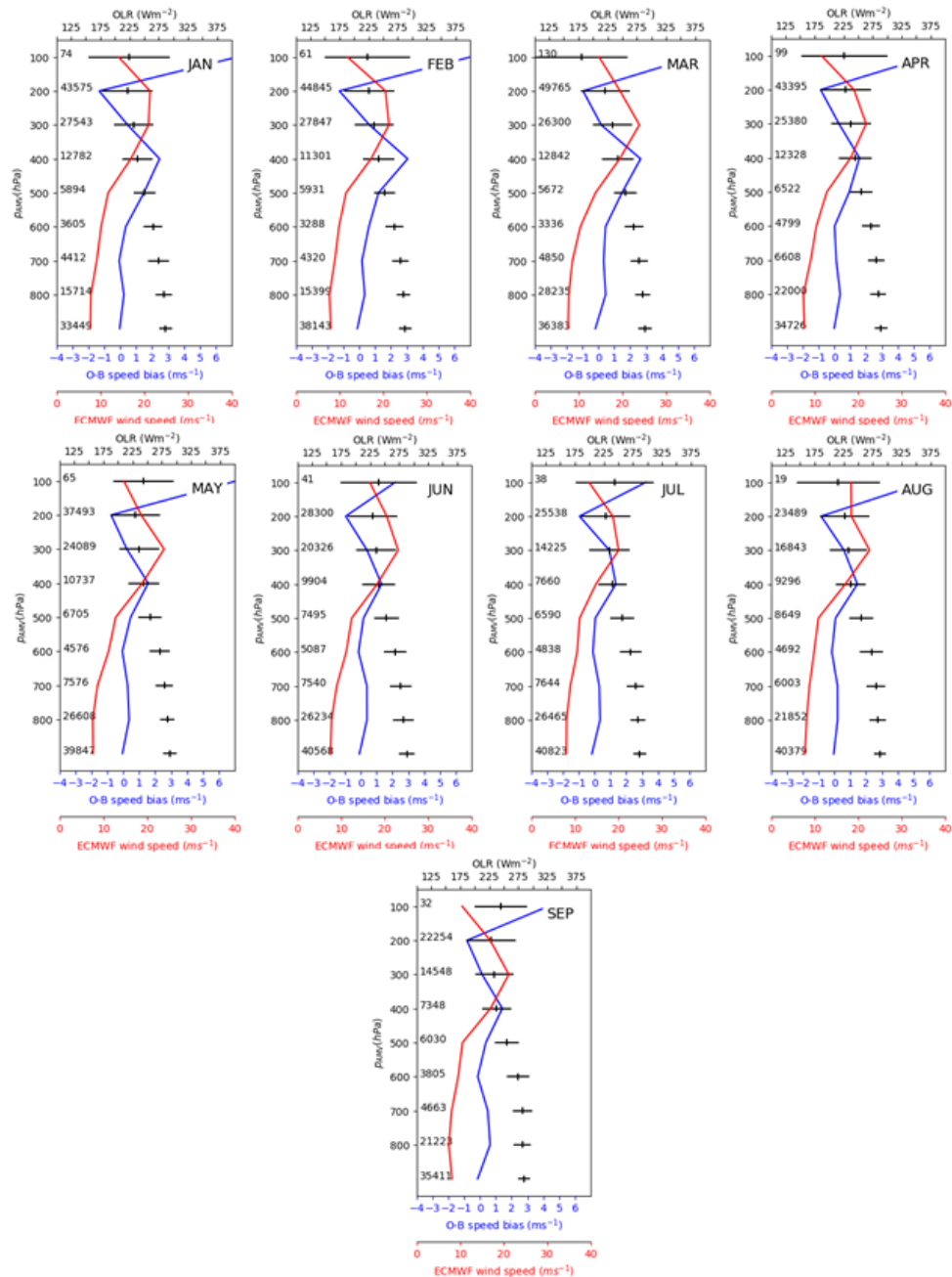
OLR provided by AIRS are collocated with AMVs if the horizontal separation between AMV and AIRS is less than 75 km and the temporal separation less than 30 min. The quality guidelines of the AIRS science team are followed and any data of low quality is discarded. OLR from AIRS/AMSU aboard AQUA and their comparison to Met10EUM and Metop AMVS and O-B speed biases are given in Figure 29 and Figure 30, respectively. Few matches are available for Metop/AIRS above 300 hPa ( $p < 300$  hPa). Below these altitudes, results resemble that of Sec. 4.5.1 (for both Met10EUM and Metop).

#### **4.5.3 OLR from FY2E/FY2G**

OLR are also available from FY2G and FY2E. However, one disadvantage of both FY2E/FY2G OLR and AMV data is the lack of any quality indicator. Nevertheless, in order to complete the suite of OLR to AMV-ECMWF wind speed comparison, results for FY2G for December 2016 and FY2E for June 2016 are presented in Figure 31. In both cases, a strong increase of the O-B speed bias with altitude is apparent. Conversely, the OLR decreases with altitude as expected. Obtained values of the mean speed differences are up to  $15 \text{ ms}^{-1}$  larger than that obtained for Met10EUM or Metop. However, parts of this large mean speed difference may be due to the lack of quality indicators.




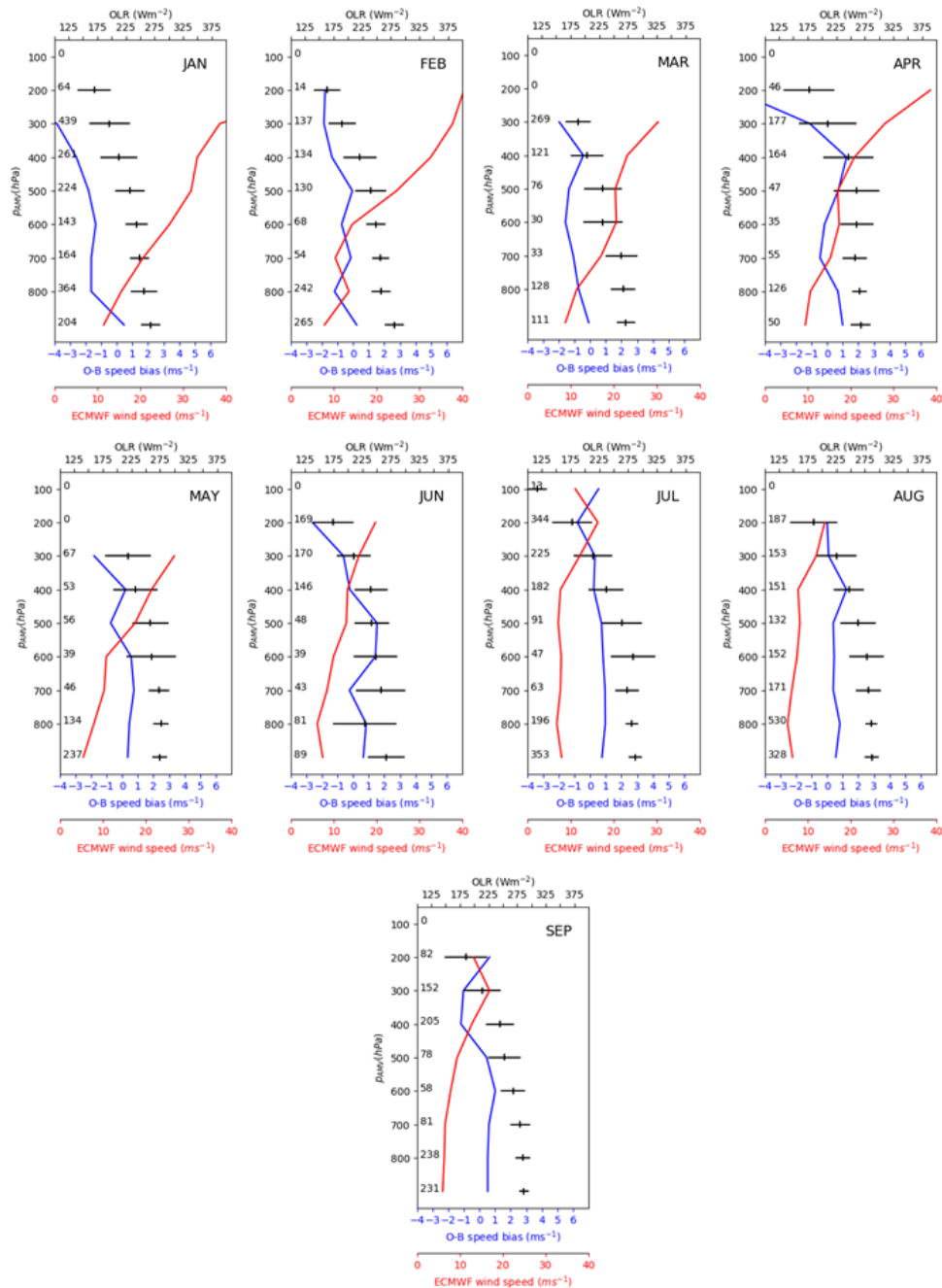
|   |  |              |
|---|--|--------------|
|  | <p align="center"><b>Study of AMV speed biases in the tropics</b></p> <p align="center"><b>Mid-term review report</b></p> <p align="center"><b>Results Task 1 - Task 3</b></p> |              |
| Reference: AMV-TN-0004-TS_Ed1_Rev1  | Date : 17/04/2019  | Page : 44/59 |




**Figure 29 : Comparison of AIRS OLR with Met10EUM AMVs. Black horizontal lines denote the mean OLR plus corresponding standard deviations. Corresponding O-B speed bias (Met10EUM-ECMWF) is shown in blue, while collocated ECMWF wind speed is shown in red.**

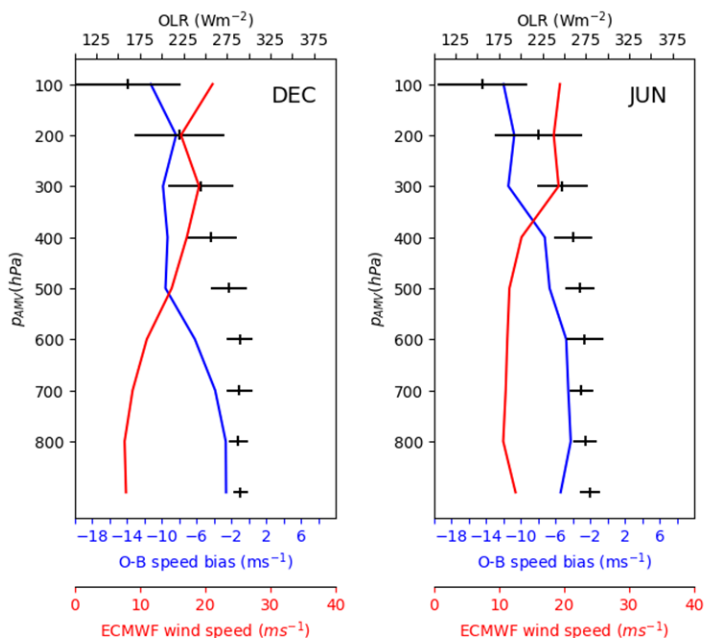


|   |  |              |
|---|--|--------------|
|  | <p align="center"><b>Study of AMV speed biases in the tropics</b></p> <p align="center"><b>Mid-term review report</b></p> <p align="center"><b>Results Task 1 - Task 3</b></p> |              |
| Reference: AMV-TN-0004-TS_Ed1_Rev1  | Date : 17/04/2019  | Page : 45/59 |



**Figure 30 : As Figure 29, but for AIRS OLR and Metop AMV.**

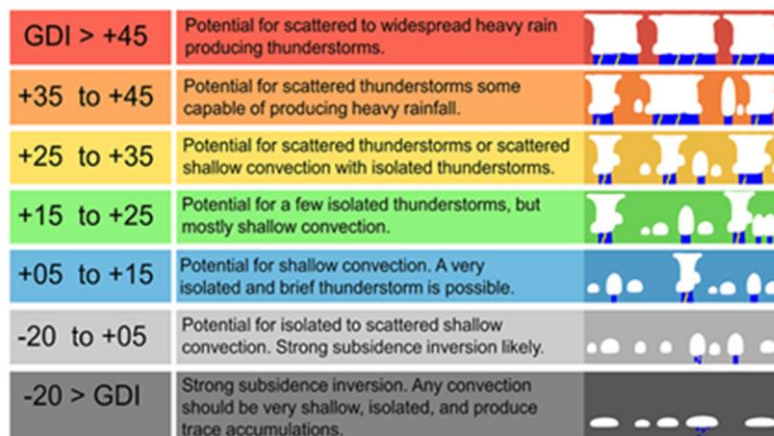
|   |  |              |
|---|--|--------------|
|  | <p align="center"><b>Study of AMV speed biases in the tropics</b></p> <p align="center"><b>Mid-term review report</b></p> <p align="center"><b>Results Task 1 - Task 3</b></p> |              |
| Reference: AMV-TN-0004-TS_Ed1_Rev1  | Date : 17/04/2019  | Page : 46/59 |



**Figure 31 : As Fig. 30 but for collocated OLR and AMV from FY2G and FY2E, respectively. (Left) Mean and standard deviation of matched FY2G OLR vs FY2G AMV-ECMWF in December 2016. (Right) Mean and standard deviation of matched FY2E OLR vs FY2E AMV-ECMWF in June 2016.**

## 4.6 GDI

Correlating mean AMV-ECWTF wind speed differences to GDI is another attempt at relating this bias to convection. GDI is described in Galvez and Davison (2016) and requires T and q at 950, 850, 700 and 500 hPa as inputs. Typical GDI values are given in Figure 32 and describe the potential for development of specific convective regimes. Note it was intended to calculate the GDI also from T and q profiles of RAOB radiosondes. However, none of the radiosondes flown in the tropics in 2016 provided a humidity profile.




**Figure 32 : Correspondence between GDI values and expected type of convection. Figure adapted from <http://www.wpc.ncep.noaa.gov/international/gdi/>**

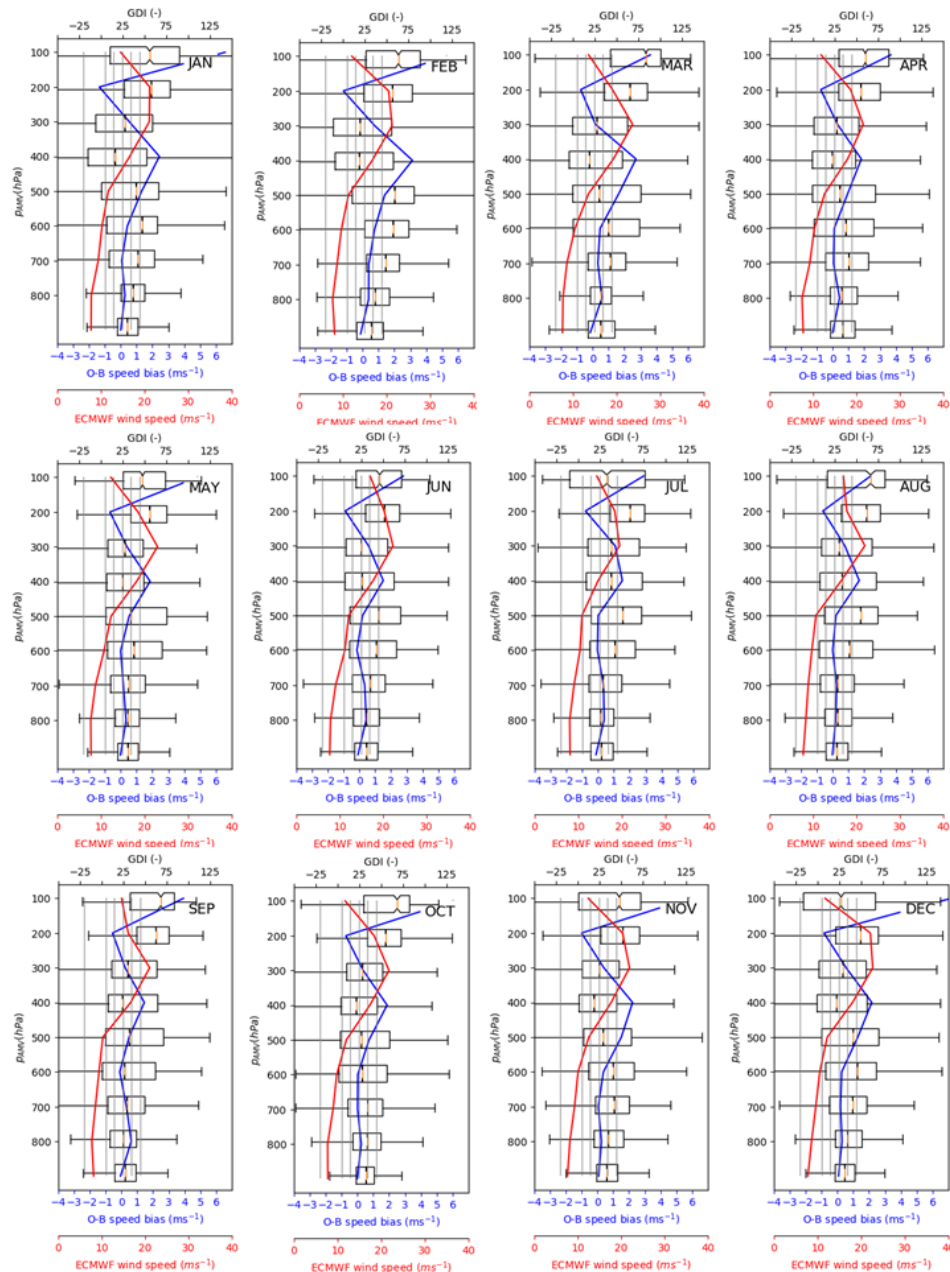
#### 4.6.1 GDI from ECMWF

Based on the collocation database established in Sec. 3, collocated T and q profiles are used to compute the GDI. Results for GDI vs O-B speed bias is given in Figure 33 for Met10EUM and in Figure 34 for Metop, respectively. In general, these figures confirm the findings of the OLR/speed bias analysis. High-level Metop AMVs are taken in stronger convective regimes than Met10EUM AMVs but no clear correlation between convection type and speed bias could be deduced.


#### 4.6.2 GDI from ATOVS

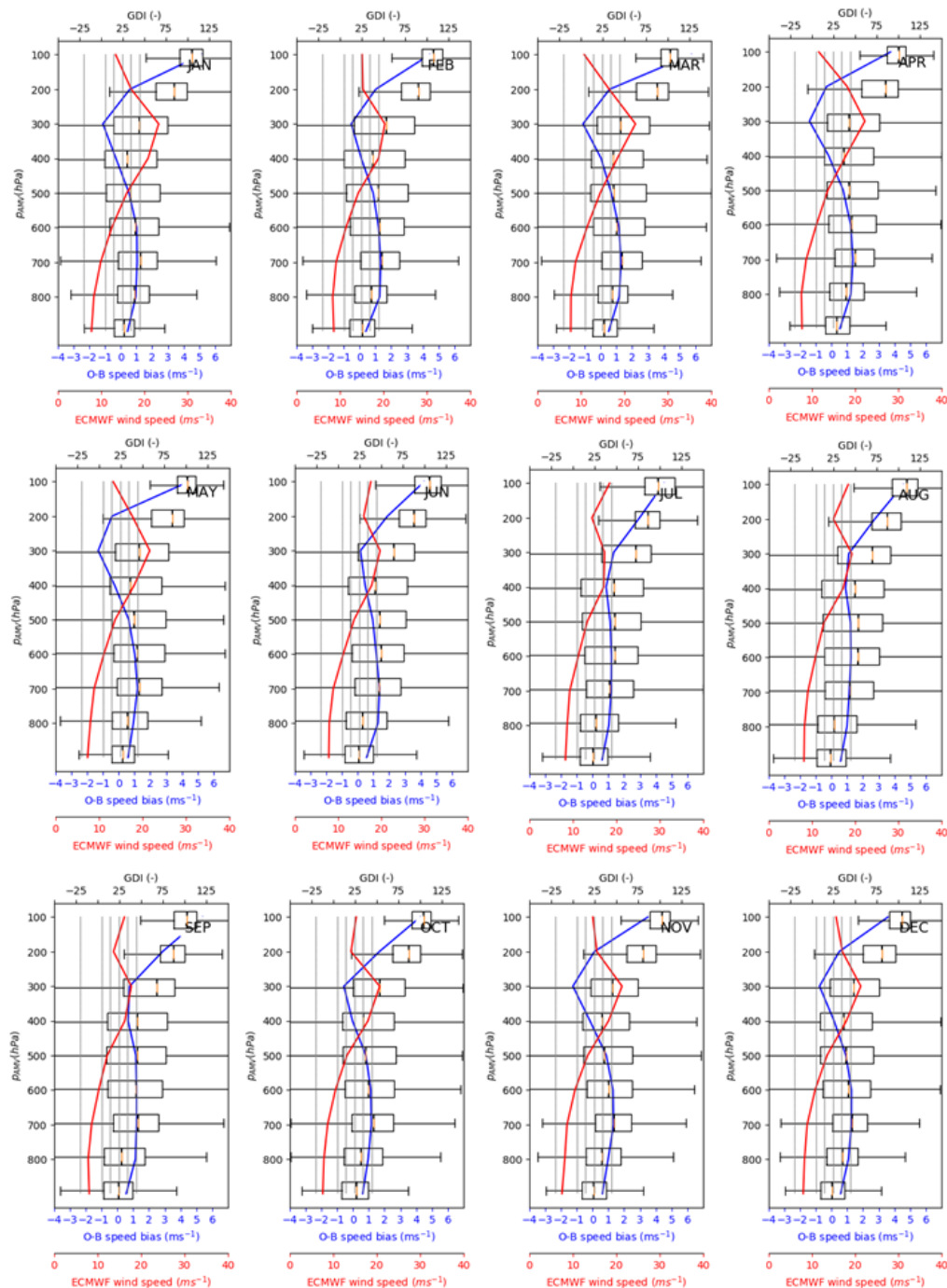
Based on the database of ECMWF and collocated Met10EUM and Metop AMVs established in Sec. 3, ATOVS T and q profiles are considered collocated if they are within a horizontal distance of 75 km and within 30 min. The quality guidelines were followed to ensure these profiles are of high quality. Results for ATOVS GDI and collocated mean speed differences are shown for Met10EUM in Figure 35 and for Metop AMVs in Figure 36. As for ECMWF OLR, GDI confirms that Metop tend to sense in stronger convective regimes, particularly above 200 hPa ( $p < 200$  hPa). However, no clear correlation between convection type and speed bias could be deduced.

|   |   |                   |
|---|---|-------------------|
|  | <p style="text-align: center;"><b>Study of AMV speed biases in the tropics</b></p> <p style="text-align: center;"><b>Mid-term review report</b></p> <p style="text-align: center;"><b>Results Task 1 - Task 3</b></p> |                   |
|   | Reference: AMV-TN-0004-TS_Ed1_Rev1  | Date : 17/04/2019 |
|   |   | Page : 48/59      |




**Figure 33 : Comparison of ECMWF GDI with Met10EUM AMVs. Box-and-whisker plots of GDI are shown for different AMV pressure levels. Each box extends from the lower to upper quartile values of the pressure differences, with a line at the median. Corresponding O-B speed bias is shown in blue, while ECMWF speeds are shown in red. The grey vertical stripes denotes the border of the different convective regimes according to Figure 32.**

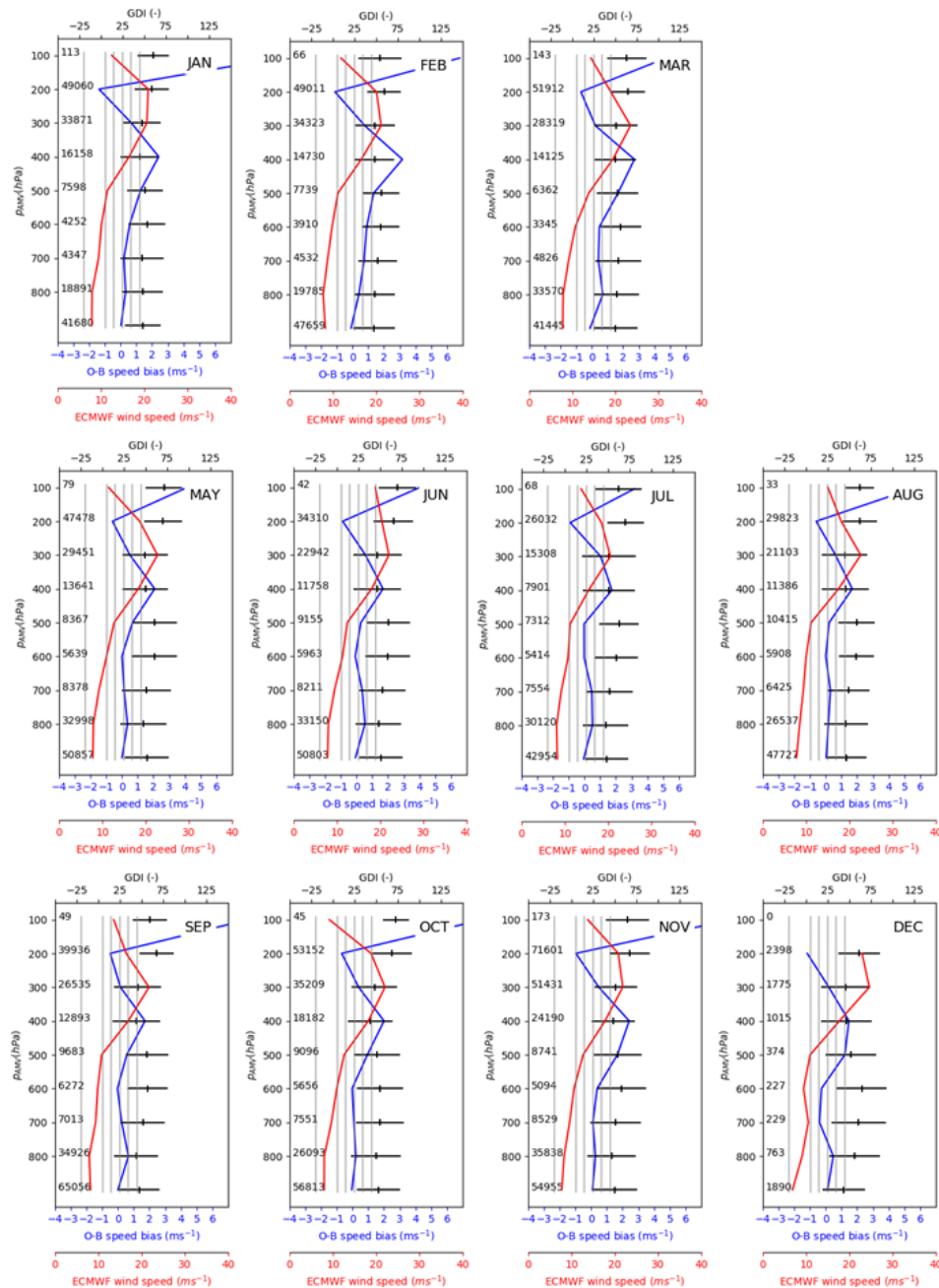
|   |  |                   |
|---|--|-------------------|
|  | <p align="center"><b>Study of AMV speed biases in the tropics</b></p> <p align="center"><b>Mid-term review report</b></p> <p align="center"><b>Results Task 1 - Task 3</b></p> |                   |
|   | Reference: AMV-TN-0004-TS_Ed1_Rev1   | Date : 17/04/2019 |
|   |  | Page : 49/59      |




**Figure 34 : As Figure 33, but for Metop AMVs.**

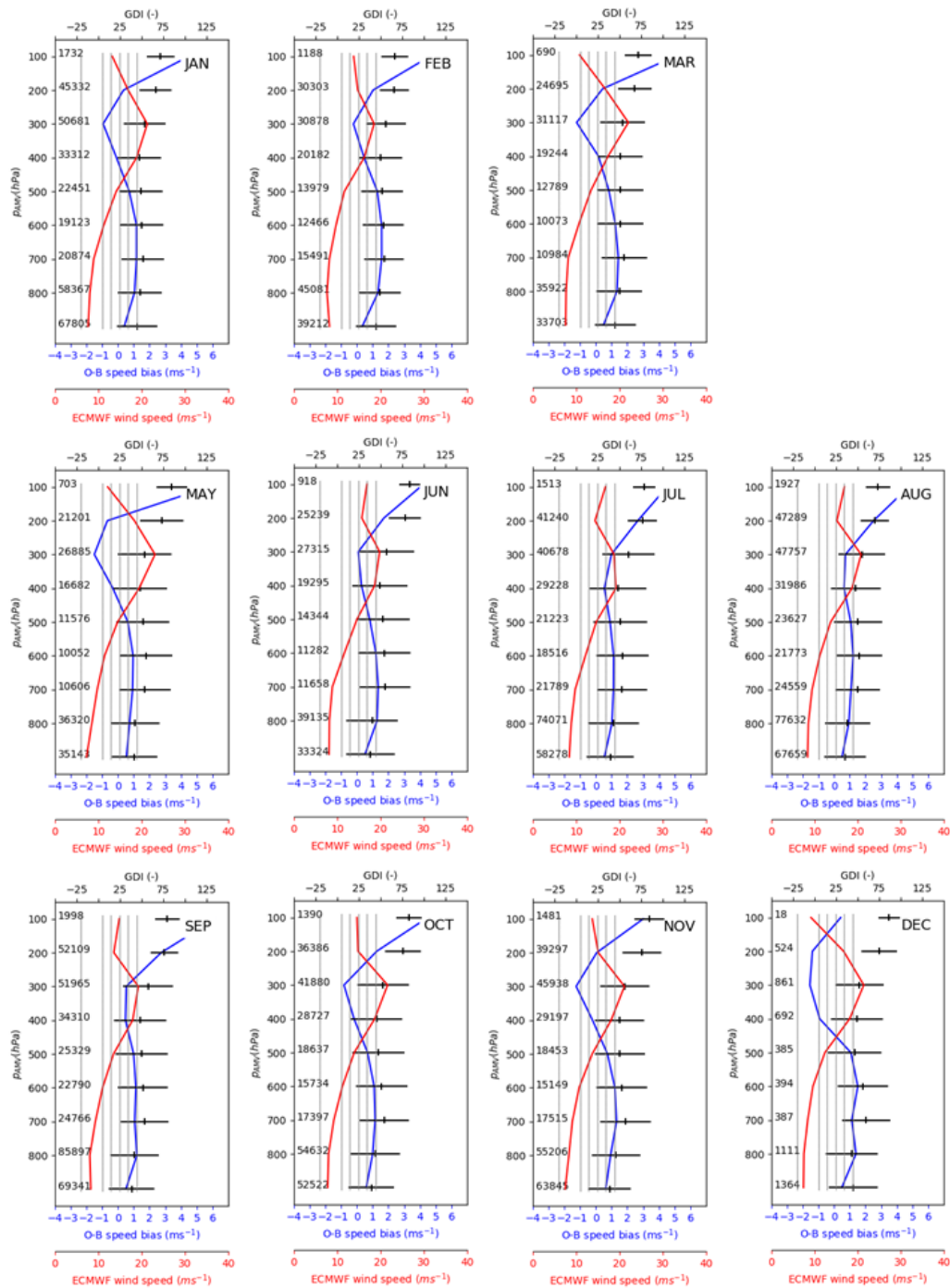


|   |   |              |
|---|---|--------------|
|  | <p style="text-align: center;"><b>Study of AMV speed biases in the tropics</b></p> <p style="text-align: center;"><b>Mid-term review report</b></p> <p style="text-align: center;"><b>Results Task 1 - Task 3</b></p> |              |
| Reference: AMV-TN-0004-TS_Ed1_Rev1  | Date : 17/04/2019   | Page : 50/59 |




**Figure 35 : Comparison of ATOVS GDI with Met10EUM AMVs. Black horizontal lines denote the mean GDI values plus corresponding standard deviations. Corresponding O-B speed bias (Met10EUM-ECMWF) is shown in blue, while ECMWF speed is shown in red. The grey vertical stripes denotes the border of the different convective regimes according to Figure 32.**

|   |  |              |
|---|--|--------------|
|  | <p align="center"><b>Study of AMV speed biases in the tropics</b></p> <p align="center"><b>Mid-term review report</b></p> <p align="center"><b>Results Task 1 - Task 3</b></p> |              |
| Reference: AMV-TN-0004-TS_Ed1_Rev1  | Date : 17/04/2019  | Page : 51/59 |



**Figure 36 : As Figure 35, but for Metop AMVs.**

|   |  |              |
|---|--|--------------|
|  | <p align="center"><b>Study of AMV speed biases in the tropics</b></p> <p align="center"><b>Mid-term review report</b></p> <p align="center"><b>Results Task 1 - Task 3</b></p> |              |
| Reference: AMV-TN-0004-TS_Ed1_Rev1  | Date : 17/04/2019  | Page : 52/59 |

## 5 SEMIVARIOGRAM

### 5.1 METHOD

The previous analysis (Speed bias as function of time of day, OLR, GDI, CLOUDSAT cloud classification) indicate little dependency of O-B speed bias on the strength and type of convection and on cloud type. Comparison of Met10AMV pressures to CALIPSO cloud top heights revealed that AMVs tend to have assigned too low altitudes at high levels. However, collocated O-B speed bias tends to be negative, which cannot be explained by having AMVs set too low in the atmosphere. Analysing the spatial variance of AMV and model speed over a region allows verifying the similarity of the wind fields (e.g. position and strength of jet). In spatial statistics, this is commonly done by plotting the semivariances as function of lag distance ("semivariogram"). The empirical semivariance  $\gamma(h)$  can be calculated according to


$$\hat{\gamma}(h) = \frac{1}{2N(h)} \sum_i^{N(h)} (z(x_i) - z(x_i + h))^2 \quad (1)$$

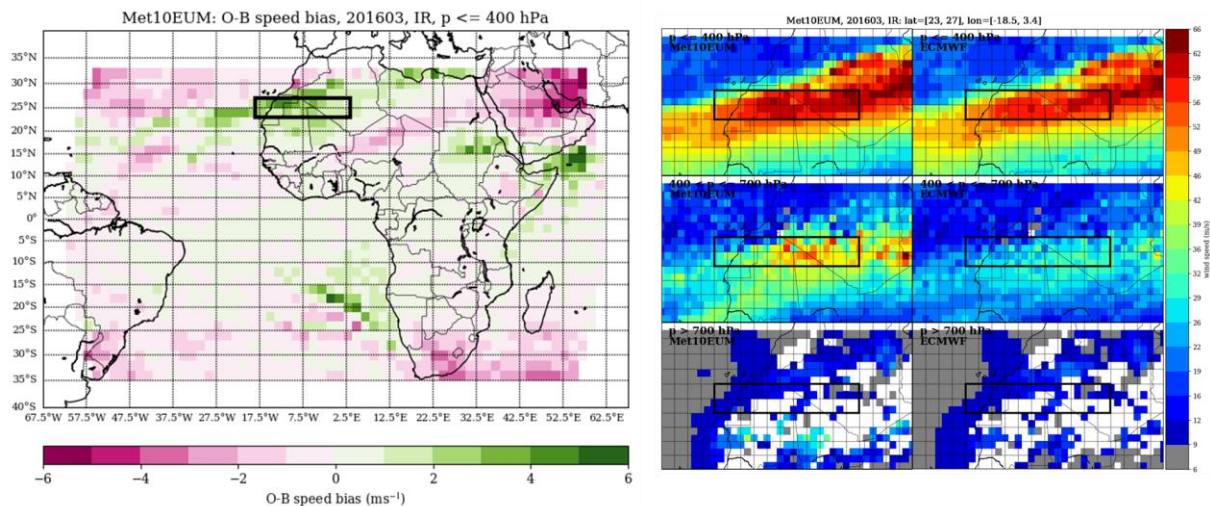
Here,  $h$  is a distance, and  $z(x_i)$  and  $z(x_i + h)$  are two data points (e.g. model wind speed at the same pressure level and time) at locations  $x_i$  and  $x_i + h$ . The  $N(h)$  term is the number of points we have that are separated by the distance  $h$ . The empirical semivariance  $\gamma(h)$  then is the sum of squared differences between values separated by a distance  $h$ . In the following, semivariograms of Metop and Met10EUM AMV and model winds will be analysed for selected cases to verify similarities/discrepancies in the wind fields.

The semivariogram analysis use the collocation data base established in Sec. 3. The ECMWF semivariances are thus comprised of purely horizontal variances at a given time, while semivariances of AMV also include a small portion of vertical variances, which are introduced by the vertical matching criterion of 25 hPa.

### 5.2 RESULTS

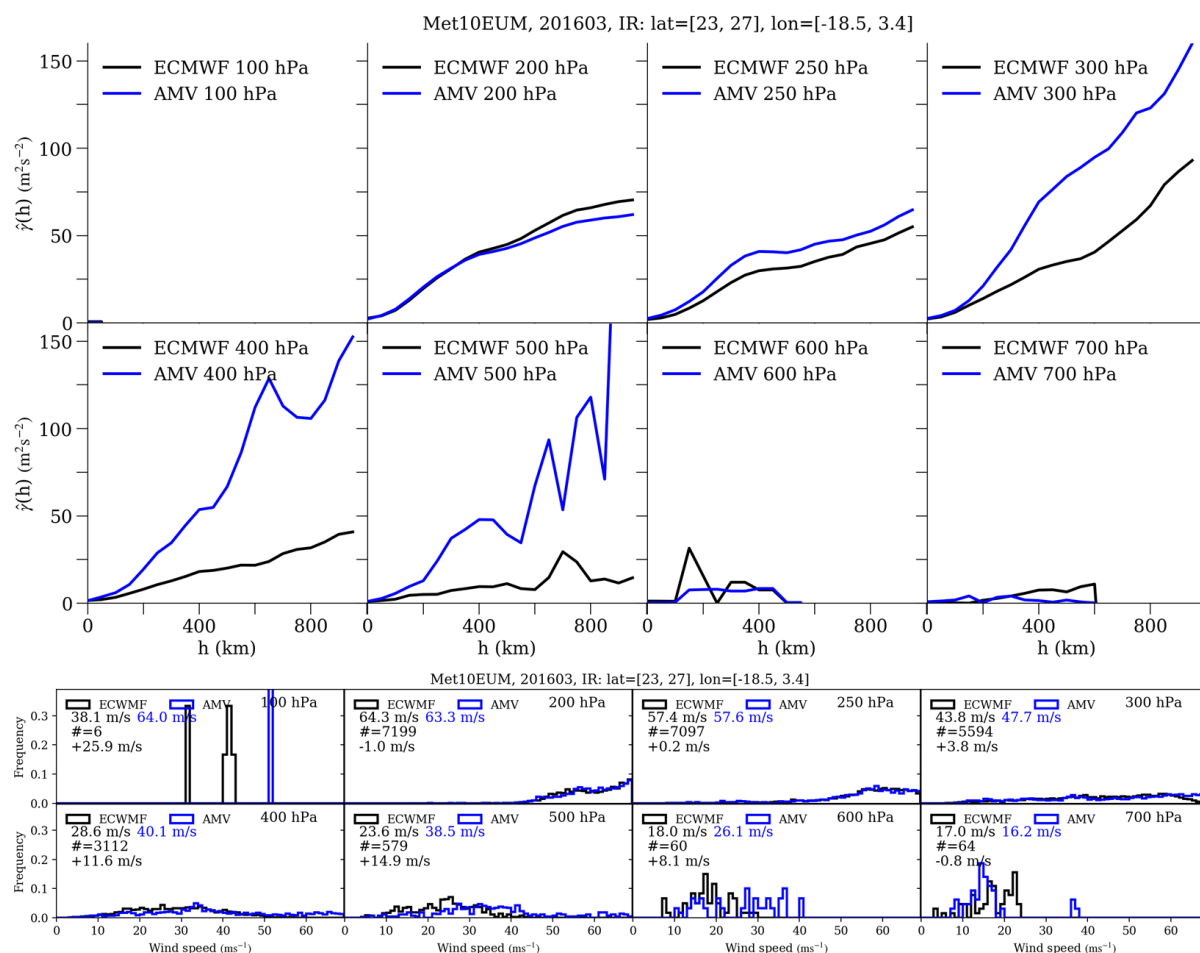
For high-levels winds, wind speed biases between Met10M and ECMWF larger than  $3 \text{ ms}^{-1}$  are frequently obtained for regions of large wind speeds. A close look at such a situation is given in Figure 37. It reveals that for Met10EUM wind speeds greater than  $60 \text{ ms}^{-1}$  appear located more south-west than for ECMWF. In addition, wind speeds greater than  $40 \text{ ms}^{-1}$  also reach to mid-levels, which is not modelled by ECMWF.

|   |  |              |
|---|--|--------------|
|  | <p align="center"><b>Study of AMV speed biases in the tropics</b></p> <p align="center"><b>Mid-term review report</b></p> <p align="center"><b>Results Task 1 - Task 3</b></p> |              |
| Reference: AMV-TN-0004-TS_Ed1_Rev1  | Date : 17/04/2019  | Page : 53/59 |



**Figure 37 : Geographic distribution of tropical Met10EUM wind speeds against collocated ECMWF winds for March 2016. (Left) O-B bias is averaged for high levels ( $p \leq 400$  hPa) and over a  $2^\circ \times 2^\circ$  latitude x longitude grid. Black square indicates a region of large wind speed discrepancies. (Right) Monthly averages of Met10EUM AMV and ECWME wind speed for high-level, mid-level and low-level winds for the black square and its surrounding are depicted.**

Semivariograms and corresponding histograms of Met10EUM and ECMWF wind speed are given in Figure 38 for selected pressure levels. The semivariograms of both Met10EUM AMV and ECMWF wind speeds for the 200 and 250 hPa level are similar, indicating similar position and strength of the jet at these levels. This is confirmed by histograms that show an almost identical distribution. By contrast, the semivariograms of Met10EUM wind speeds at 300 and 400 hPa show a much stronger increase of variance with distance than ECMWF, indicating that different spatial structures of wind are obtained and mean speed differences amount to  $4 - 11 \text{ ms}^{-1}$  (AMV faster than ECMWF).



**Figure 38 : Semivariograms and histograms of Met10EUM AMV and model wind for different pressure levels for the black square region of Figure 37. (Upper panel) Semivariance  $\gamma$  for AMV (blue) and model wind (black) as function of lag distance  $h$  for selected pressure levels. (Lower panel) Corresponding histograms of AMV (blue) and model wind (black). The numbers indicate the mean of the histograms (blue for AMV histogram, black for model wind), and observed O-B speed bias (AMV-Model). # denotes the sample size.**

In Figure 39, the reverse situation of ECMWF reporting larger wind speeds than Met10EUM AMV observations at high-levels is depicted. ECMWF winds larger  $30 ms^{-1}$  are modelled for a region spreading from the Liberian coast to Ghana. By contrast, Met10EUM does not observe such wind speeds for southwestern part of the region, leading to negative mean speed differences between AMV and model winds at high-levels. The semivariogram (Figure 40) reveals that ECMWF exhibits stronger increase of variances with distance than Met10EUM at 200 hPa. This pattern, however, changes at the 300 hPa, where AMVs tend to exhibit higher semivariances than model winds. This change in semivariance pattern is accompanied by a change in the sign of the O-B speed bias. For lower altitudes,




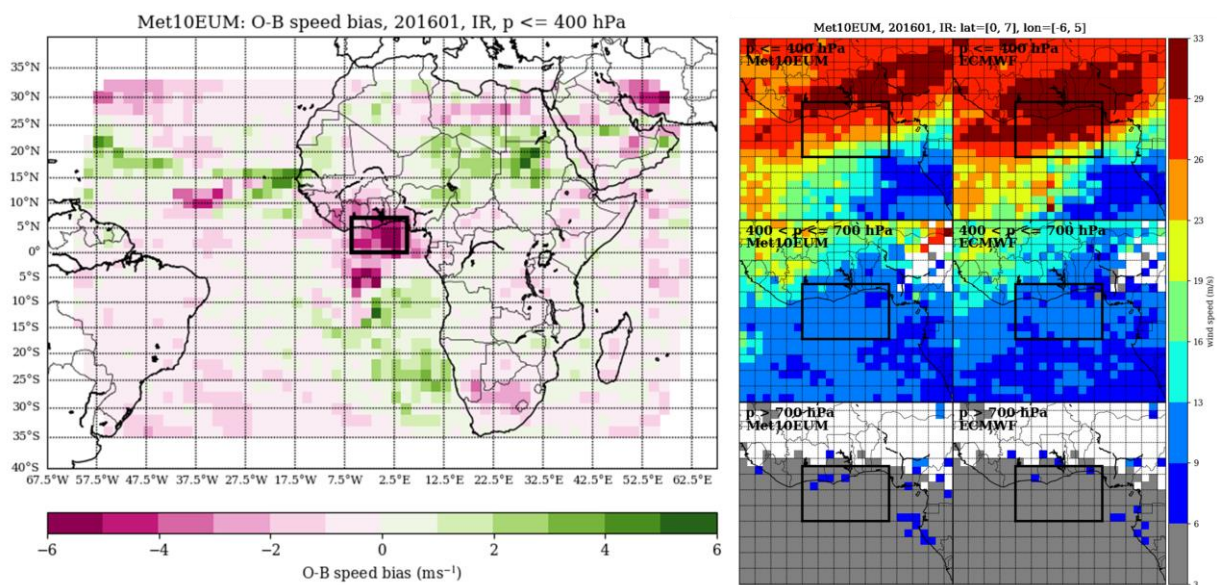
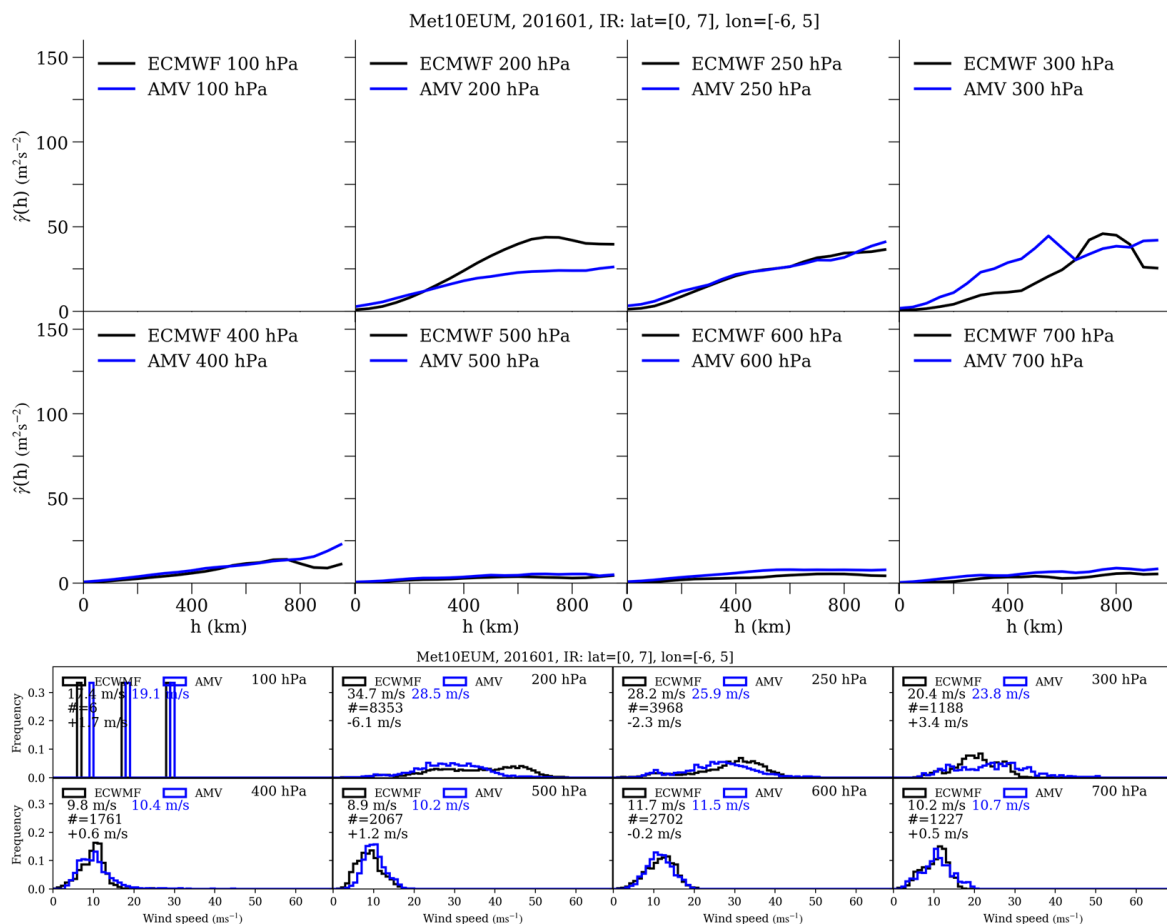
|   |  |              |
|---|--|--------------|
|  | <p align="center"><b>Study of AMV speed biases in the tropics</b></p> <p align="center"><b>Mid-term review report</b></p> <p align="center"><b>Results Task 1 - Task 3</b></p> |              |
| Reference: AMV-TN-0004-TS_Ed1_Rev1  | Date : 17/04/2019  | Page : 55/59 |

Figure 40 shows a rather homogeneous distribution of the wind speed. Consequently, the semivariograms and histograms are very similar. Reported wind speed biases are between  $-0.2$  and  $1.2 \text{ ms}^{-1}$ .




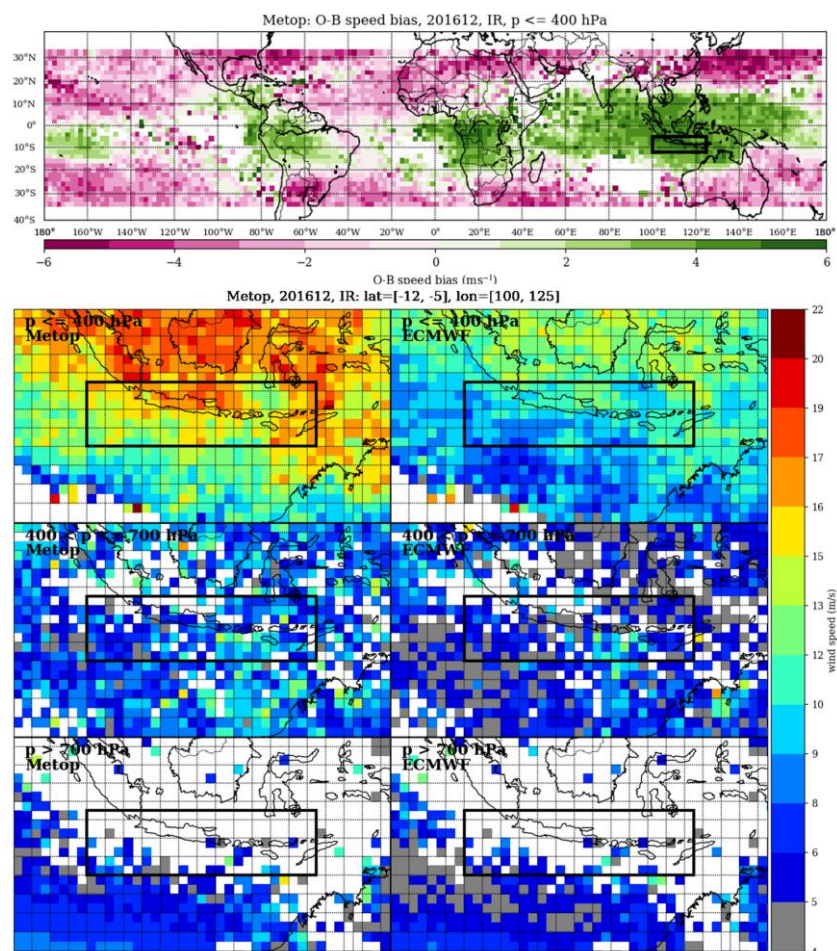
**Figure 39 : Geographic distribution of tropical Met10EUM wind speeds against collocated ECMWF winds for January 2016. (Left) O-B bias is averaged for high levels ( $p \leq 400 \text{ hPa}$ ) and over a  $2^\circ \times 2^\circ$  latitude x longitude grid. Black square indicates a region of large wind speed discrepancies. (Right) Monthly averages of Met10EUM AMV and ECWMF wind speed for high-level, mid-level and low level winds for the black square and its surrounding.**



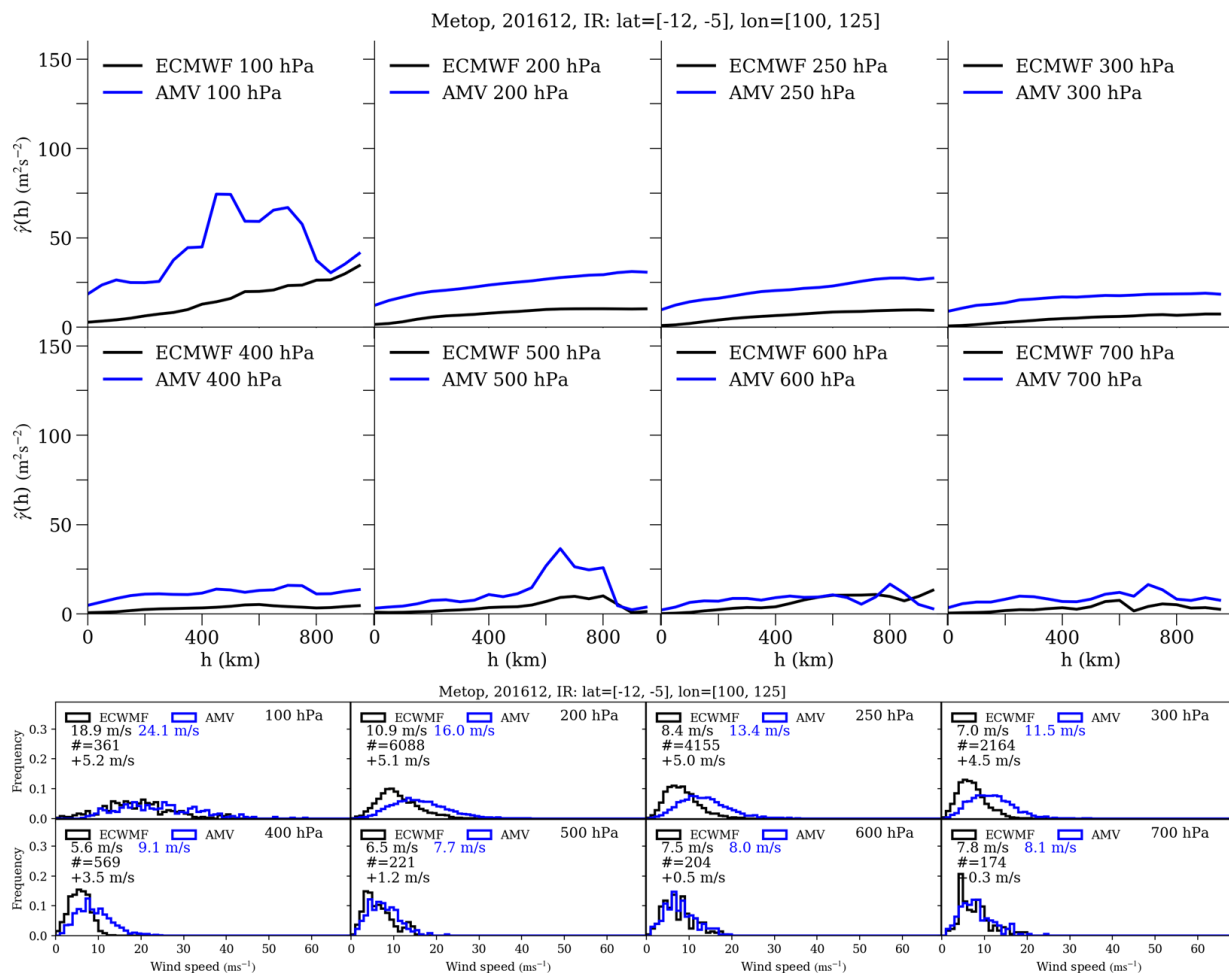
**Figure 40 : As Figure 38, but for the black square region of Figure 39.**

Figure 41 shows as an example of large O-B speed bias (Metop-ECWMF) of  $> 4 \text{ ms}^{-1}$  over Indonesia for high-levels. Corresponding semivariograms and histograms for selected pressure levels are displayed in Figure 42. For all levels, Metop exhibits larger semivariograms and thus smaller spatial autocorrelation than ECMWF and higher average wind speed than ECMWF. At 100 hPa, the semi-variances for lag distances of 400 to 800 km is particularly large. In contrast to Met10EUM, Metop exhibits already semivariograms  $> 0 \text{ m}^2\text{s}^{-2}$  at lag distances close to 0 km, which represent wind speed variations at very small scale and within the 25 hPa vertical match criterion.

|   |  |              |
|---|--|--------------|
|  | <p align="center"><b>Study of AMV speed biases in the tropics</b></p> <p align="center"><b>Mid-term review report</b></p> <p align="center"><b>Results Task 1 - Task 3</b></p> |              |
| Reference: AMV-TN-0004-TS_Ed1_Rev1  | Date : 17/04/2019  | Page : 57/59 |




**Figure 41 : Geographic distribution of tropical Metop wind speeds against col-located ECMWF winds for December 2016. (Top) O-B bias is averaged for high levels ( $p \leq 400$  hPa) and over a  $2^\circ \times 2^\circ$  latitude x longitude grid. Black square over Indonesia indicates a region of large wind speed discrepancies. (Bottom) Monthly averages of Metop AMV and ECWMF wind speed for high-level, mid-level and low level winds for the black square and its surrounding.**



**Figure 42 : As Figure 38, but for the black square region of Figure 41.**



|   |  |              |
|---|--|--------------|
|  | <p align="center"><b>Study of AMV speed biases in the tropics</b></p> <p align="center"><b>Mid-term review report</b></p> <p align="center"><b>Results Task 1 - Task 3</b></p> |              |
| Reference: AMV-TN-0004-TS_Ed1_Rev1  | Date : 17/04/2019  | Page : 59/59 |

## 6 SUMMARY AND CONCLUSIONS

AMVs from Met10EUM and Metop IR imagery were compared to hourly forecast winds from ECMWF to check the degree of agreement between model and satellite observations. The pattern of O-B wind speed bias obtained from Met10EUM and Metop AMVs differs at high-level. For AMVs derived from the geostationary Meteosat-10 satellite, areas of positive O-B speed biases  $> 3 \text{ ms}^{-1}$  commonly coincide with the location of the subtropical jet that migrates with the changing position of the thermal equator. Other areas of large wind speed discrepancies ( $> 3 \text{ ms}^{-1}$ ) are found over desert sites and oceans, potentially attributable to the lack of observational data to constrain appropriately the NWP model. For AMVs obtained from Metop, a different spatial pattern at this level was obtained. O-B speed bias was negative regions exhibiting mean wind speeds greater than  $30 \text{ ms}^{-1}$ , while positive O-B speed biases were obtained for low wind speed regions around the equator.

At mid-levels, large differences of  $> 6 \text{ ms}^{-1}$  were found over the Sahara desert in northern hemisphere winter for Met10EUM, which is explained by AMV altitudes set too low in the atmosphere. For Metop, observed pattern of wind speed discrepancies resemble that observed at high levels. However, observed amplitude of wind speed differences is smaller, coinciding with smaller wind speeds at these altitudes. At low-levels, Met10EUM agree with ECMWF within  $1 \text{ ms}^{-1}$ , except for certain arid locations in Northern Africa. For Metop, the observed O-B speed biases are typically of similar magnitude as for Met10EUM.

Comparing observed O-B speed biases to parameters describing strength and type of convection such as GDI, OLR, to CLOUDSAT cloud type as well as to the diurnal cycle of convection revealed no clear dependency of the O-B speed bias to these parameters. However, it is interesting to note that Metop tends to sense in stronger convective regimes than Met10EUM, which may be explained by the fact that Metop also senses over Monsoon regions of South East Asia and its temporal sampling. In contrast to Met10EUM, it overpasses tropical locations once in the morning and once in the evening.

Comparison to CALIPSO cloud top heights was only possible to Met10EUM AMV pressures. Overall, pressures assigned to AMVs are larger than collocated CALIPSO cloud top heights. Parts of this pressure difference ( $\Delta p = p_{\text{AMV}} - p_{\text{CALIPSO}}$ ) may be attributed to the AMVs representing actual winds below the cloud top (Folger and Weissmann, 2014). Despite  $\Delta p > 0$ , observed O-B speed biases are negative for high levels (about  $-1 \text{ ms}^{-1}$ ) above 300 hPa ( $p < 300 \text{ hPa}$ ). Thus, erroneous height assignment unlikely explains observed O-B speed biases at these levels.

Lastly, semiovariograms were computed for regions where monthly wind speed discrepancies were large in order to verify the spatial structure of observed and model winds. Large O-B speed biases (both negative and positive biases) are observed when semivariances obtained for AMVs vary widely from those obtained from ECMWF, indicating that the wind fields' spatial structure differ substantially, e.g. the location and extend of the subtropical jet. In such cases, one cannot rule out completely that the origin of the speed bias is due to deficiencies in the model wind.

So far, only mean statistics (mean differences averaged over season or month, geographic distribution of monthly O-B speed biases averaged for high-, mid- and low levels) have been deduced. As a next step, it is planned to study in depth cases where observed fast (slow) O-B speed bias and altitude is assigned too high (low). Interesting regions in this sense are the Western Pacific Boiler box for Metop or the Indian Ocean south of Madagascar for both Metop and Met10EUM. It should be checked if the structure of zonal and meridional wind component between model and satellite observation is similar. For instance, if  $u$  structure is similar between AMV and model but differences in the  $v$  component are apparent, the location of the jet differs in both data sets.